

SEPTEMBER 1991

# HEWLETT-PACKARD JOURNAL



## Contents:

SEPTEMBER 1981 Volume 32 • Number 9

- 3 A Reliable, Accurate CO<sub>2</sub> Analyzer for Medical Use**, by Rodney J. Solomon *A novel sensor design and digital processing make this instrument reliable and easy to use.*
- 8 A Miniature Motor for the CO<sub>2</sub> Sensor**, by Edwin B. Merrick *The rotor contains optical elements, is the size of a coin, and rotates at 2400 r/min.*
- 12 An End-Tidal/Respiration-Rate Algorithm**, by John J. Krieger *An infrared absorption signal is processed digitally to yield CO<sub>2</sub> level and rate of breathing.*
- 16 In-Service CO<sub>2</sub> Sensor Calibration**, by Russell A. Parker and Rodney J. Solomon *Quick and easy calibration is essential for a medical instrument.*
- 19 Making Accurate CO<sub>2</sub> Measurements**, by John J. Krieger *This system produces accurate gas mixtures for CO<sub>2</sub> sensor calibration.*
- 22 A Versatile Low-Frequency Impedance Analyzer with an Integral Tracking Gain-Phase Meter**, by Yoh Narimatsu, Kanuyaki Yagi, and Takeo Shimizu *Complex component and circuit evaluations are done automatically at frequencies from 5 Hz to 13 MHz.*
- 29 A Fast, Programmable Pulse Generator Output Stage**, by Peter Aue *Here's a 100-MHz pulse generator with fast transition times for testing fast logic families.*

## In this Issue:



Carbon dioxide (CO<sub>2</sub>) builds up in our blood as a byproduct of metabolism and we must eliminate it from our bodies or die. Some is eliminated through the kidneys and a small amount goes out through the skin, but most is carried to the lungs and exhaled. As metabolic needs increase, the body's built-in control system makes us breathe harder to keep the level of carbon dioxide in the blood at a safe level. When this control system isn't working, as is the case for a patient on a mechanical ventilator, the physician must monitor the level of CO<sub>2</sub> in the patient's blood and adjust the respiration rate accordingly. Rather than draw blood samples periodically, the physician may elect to monitor the level of CO<sub>2</sub> in the patient's exhaled breath. The expired CO<sub>2</sub> is normally a good indicator of blood CO<sub>2</sub>.

Capnometers, or CO<sub>2</sub> analyzers, have been used for 30 years to monitor ventilated patients. They are also used in operating rooms to monitor the general physiological status of anesthetized patients, and they are used in pulmonary laboratories to help assess how well a patient's lungs are functioning. However, there have been problems. Many capnometers that measure expired CO<sub>2</sub> on a continuous basis sample the expired gas through a small tube. This tube often becomes clogged with condensed moisture and secretions. This and other problems make these instruments somewhat unstable and unreliable.

The new HP Model 47210A Capnometer, featured on the cover of this issue, eliminates the problems of earlier instruments and makes a major contribution to the field of medical gas monitoring. It makes its measurements directly on the breathing gas, using an airway adapter with a snap-on infrared sensor. The approach is simple and reliable. Inside the instrument, a microcomputer takes information from the sensor, processes it, corrects for the influence of water vapor, oxygen, and nitrous oxide, and displays various measures of CO<sub>2</sub> and the respiration rate. Alarms alert medical personnel if preset limits are exceeded. Calibration, when necessary, is fast and easy. The design of the 47210A Capnometer is discussed on pages 3 to 21.

The other two articles in this month's issue describe the design of instruments that are related to former Hewlett-Packard Journal cover subjects. Model 4192A Low-Frequency Impedance Analyzer, page 22, is a close relative of our January 1980 cover subject, Model 4191A Radio-Frequency Impedance Analyzer. Both of these instruments make fundamental measurements on basic electronic components such as resistors, capacitors, and transistors and on electronic devices such as telecommunications filters, audio and video circuits, and integrated circuits. Model 4192A can test these devices at frequencies as low as 5 hertz or as high as 13 megahertz and can operate under computer control in an automated system. It can, for example, easily and automatically characterize resonators and filters such as quartz crystals, ceramic and mechanical filters, sonar cells, and piezoelectric buzzers. This class of devices has been difficult to measure efficiently and accurately by other means.

Model 8161A Pulse Generator, page 29, is a faster relative of our May 1979 cover subject, Model 8160A. Today's very fast digital integrated circuits are capable of switching between voltage levels in as little as a few thousandths of a millionth of a second. Model 8161A generates fast, accurate voltage pulses or staircases for testing these circuits. Its output voltage level, pulse rate, and switching speed are completely programmable. It'll be used in research, production, and incoming inspection of fast integrated circuits and products that use them.

-R. P. Dolan

Editor, Richard P. Dolan • Associate Editor, Kenneth A. Shaw • Art Director, Photographer, Arvid A. Danielson  
Illustrator, Nancy S. Vanderbloom • Administrative Services, Typography, Anne S. LoPresti • European Production Manager, Dick Leeksma

# A Reliable, Accurate CO<sub>2</sub> Analyzer for Medical Use

*Measuring the amount of carbon dioxide in a patient's breath is an important medical diagnostic tool. This instrument makes the measurement quickly and easily without cumbersome calibration requirements.*

by Rodney J. Solomon

**C**ARBON DIOXIDE (CO<sub>2</sub>) is one byproduct of human metabolism. Accumulation of this gas by the body leads to a shift in intracellular acidity which is incompatible with life. Elimination of CO<sub>2</sub> occurs mainly through blood transport to the lungs, although some CO<sub>2</sub> is eliminated through the kidney and a small amount is passed through the skin. Being able to measure the partial pressure of carbon dioxide (PCO<sub>2</sub>) in the patient's inhaled and exhaled breath is important because it allows the clinician to predict the arterial blood CO<sub>2</sub> concentration and thus adequacy of ventilation (breathing).

The HP Model 47210A Capnometer shown in Fig. 1 is designed to make these measurements easily and accurately without causing discomfort to the patient. The patient's breath is inhaled and exhaled through an airway that has an infrared source mounted on one side and an infrared detector mounted on the opposite side. The instrument measures the amount of infrared radiation absorbed by the

patient's breath to determine the partial pressure of CO<sub>2</sub> present. This direct measurement is done quickly and noninvasively.

The new capnometer is very useful for monitoring patients whose breathing is being done for them by a mechanical ventilator. Normally, someone who is breathing spontaneously has a natural feedback system for controlling blood PCO<sub>2</sub> level. As the person's metabolic needs increase, so does the respiration rate to maintain the blood PCO<sub>2</sub> at a constant value (usually around 40 mmHg for a normal person). For a patient on a mechanical ventilator, the physician who adjusts the ventilation controls the level of CO<sub>2</sub> in the patient's blood. The physician may use the patient's expired CO<sub>2</sub> level instead of blood gas analysis for controlling ventilation. The expired CO<sub>2</sub> reading is immediate, while with blood gas analysis, there may be a delay of a dozen minutes or so.

Arterial blood concentration of CO<sub>2</sub> is the primary



**Fig. 1.** The HP Model 47210A Capnometer noninvasively measures breath CO<sub>2</sub> content to provide accurate monitoring of a patient's breathing in operating, recovery, and respiratory care areas. Its accuracy, ease of use, and simple calibration also make it useful for pulmonary laboratory evaluations.

stimulus for respiratory control. That is, we are driven to eliminate carbon dioxide, not to acquire oxygen. Monitoring the CO<sub>2</sub> concentration in the exhaled breath and comparing that value to the CO<sub>2</sub> concentration of a drawn arterial blood gas sample can be used to make a determination of the ability of the lung to eliminate CO<sub>2</sub>. Additional diagnostic information can be gleaned from an examination of the CO<sub>2</sub> partial-pressure waveform as function of time.<sup>1</sup>

Carbon-dioxide analyzers and capnography, the study of the PCO<sub>2</sub> waveform, have been used since the early 1950s to assess patient condition. These analyzers use a nondispersive infrared technique whereby all radiation from an emitter is passed through a gas sample and the energy absorbed at the wavelength of interest is measured. In the infrared radiation region a number of gases have absorption bands (see box at right). Carbon dioxide has a strong absorption band centered around a wavelength of 4.26 μm. The energy absorption is primarily a function of CO<sub>2</sub> concentration and total radiation path length. There are other influences on the total energy absorbed such as total gas pressure, temperature and presence of other gases.

### Some Problems

CO<sub>2</sub> analyzers have had a number of problems which can make routine monitoring difficult. Most CO<sub>2</sub> analyzers operate on a sampling technique. A gas sample is drawn via a capillary tube to the analyzer from the plumbing used to connect the patient to a ventilator. This capillary tube is prone to clogging from sputum and water vapor. In addition, the instrument requires an air pump and flow regulators, and contamination has to be removed from the gas before it enters the sample chamber. The small passages and traps in such a system can make it difficult to maintain adequate cleanness. Instrument calibration, usually needed quite frequently, is done by using gas from pre-mixed cylinders. This is cumbersome, time-consuming and subject to operator error.

## Infrared Absorption

The measurement technique is based on the absorption of infrared radiation by gases having polyatomic assymmetric molecules. That is, water vapor (H<sub>2</sub>O), carbon dioxide (CO<sub>2</sub>), carbon monoxide (CO), and nitrous oxide (N<sub>2</sub>O) will absorb infrared whereas symmetrical binary gas molecules such as oxygen (O<sub>2</sub>) and nitrogen (N<sub>2</sub>) will not. The absorption bands for various gases in the infrared spectrum from 2 to 10 micrometres are shown in Fig. 1. Note that CO<sub>2</sub> has a strong absorption band for the infrared wavelengths from 3.5 to 4.7 micrometres. By using a bandpass filter to eliminate the other infrared wavelengths emitted by the infrared source in the 14360A Sensor the detector can measure the absorption caused by the amount of CO<sub>2</sub> present in a gas.

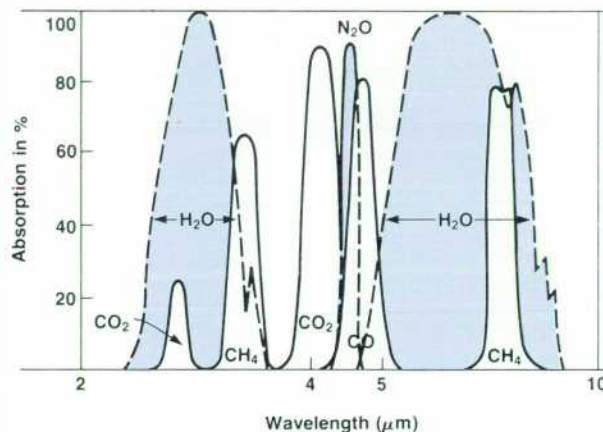


Fig. 1. Infrared absorption bands for infrared radiation wavelengths from 2 to 10 micrometres.

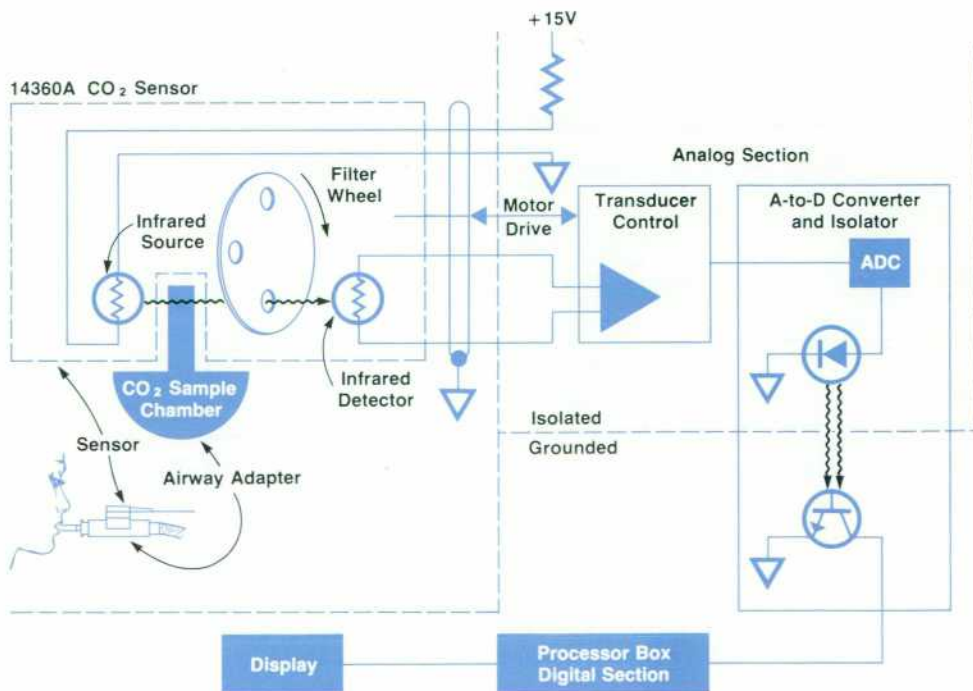
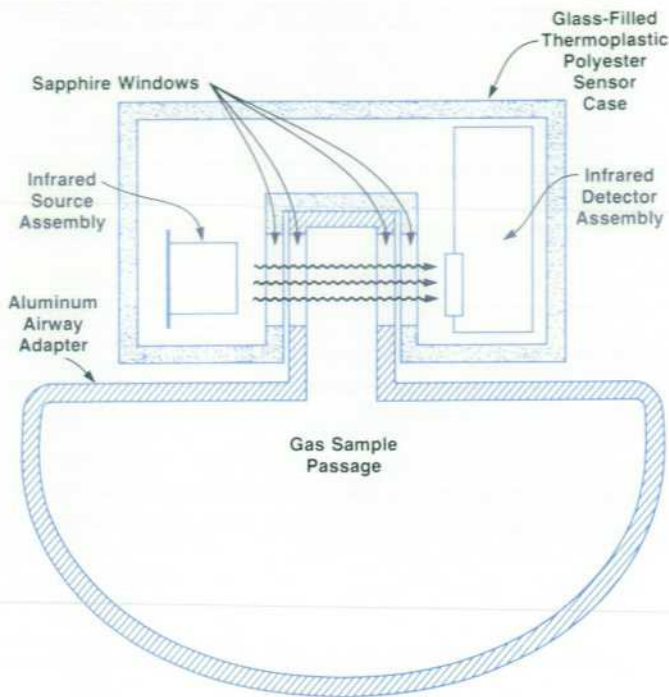


Fig. 2. Block diagram of the 47210A Capnometer. The output from the CO<sub>2</sub> sensor is controlled, amplified, and converted to digital data by the analog section in the processor box. This data is optically coupled to the rest of the processor box to be analyzed and displayed.



**Fig. 3.** Cross section of the airway adapter and sensor assembly. The sensor body contains all of the infrared components required to measure the infrared absorption of the patient's breath passing through the airway adapter.

The 47210A CO<sub>2</sub> analyzer was developed to alleviate the problems with presently available instruments. In particular:

- The small sampling tube is a trouble spot and is avoided.
- The method of instrument calibration eliminates the need for unwieldy gas cylinders.
- The stability of measurement is adequate to allow confident use for extended periods of time.
- The instrument is easy to use in a monitoring application because the complex compensation routines are performed by the instrument rather than by the operator.

The 47210A Capnometer provides the above features by making some significant changes in the basic measurement approach. A simplified block diagram of the 47210A is shown in Fig. 2.

The 47210A consists of an airway adapter, a sensor, and a processor box. The airway adapter, a hollow aluminum casting with sapphire windows, is inserted in series with the ventilator plumbing. The sensor is snapped over the airway adapter windows (Fig. 3), and the measurement is made directly on the artificial airway through which the patient is breathing (Fig. 4). This sensor contains all the optical components necessary to make the infrared measurement and is connected to the processor box by a cable 2.44 metres long. The processor box powers the sensor, processes the return signal, and presents the data via LED (light-emitting diode) displays. A simple, self-contained calibration system attached to the processor box substitutes a foolproof method for a previously difficult and potentially error-inducing calibration procedure using premixed gases. The microprocessor in the processor box performs numerous tasks that greatly simplify the use of the system. Compensations for interfering gases and total pressure are performed by the processor rather than by the operator.

### Design Goals

The fundamental approach of placing all the infrared components at the patient end of the cable offers many advantages over the sampling tube approach. The "on airway" concept is not, however, without its share of problems. The sensor must be small, rugged, lightweight, and easily cleaned, and perhaps most important, must help isolate the processor box from any high voltages caused by the use of defibrillation equipment. It also should not be a shock hazard for the patient. If a patient makes contact with a piece of equipment such as a motorized bed that has a defective ac line connection, a current can flow through the patient if the patient is grounded. The goal is to assure that the CO<sub>2</sub> analyzer does not provide either the ac source or the grounded path for the patient.

The airway adapter must be rugged and lightweight. It must be sterilizable and the infrared path length must be stable and consistent from unit to unit to minimize the total system error. Mating the airway adapter to standard ventilation plumbing must be simple and reliable.

The variability of the infrared components in the sensor must be compensated by the processor box. If the goal of a simple calibration scheme is to be realized, the processor box must be more than just a power supply for the sensor and a simple analog-to-digital (A-to-D) converter. The effects of interfering gases and total pressure variation (altitude) on the CO<sub>2</sub> measurement mean additional process-

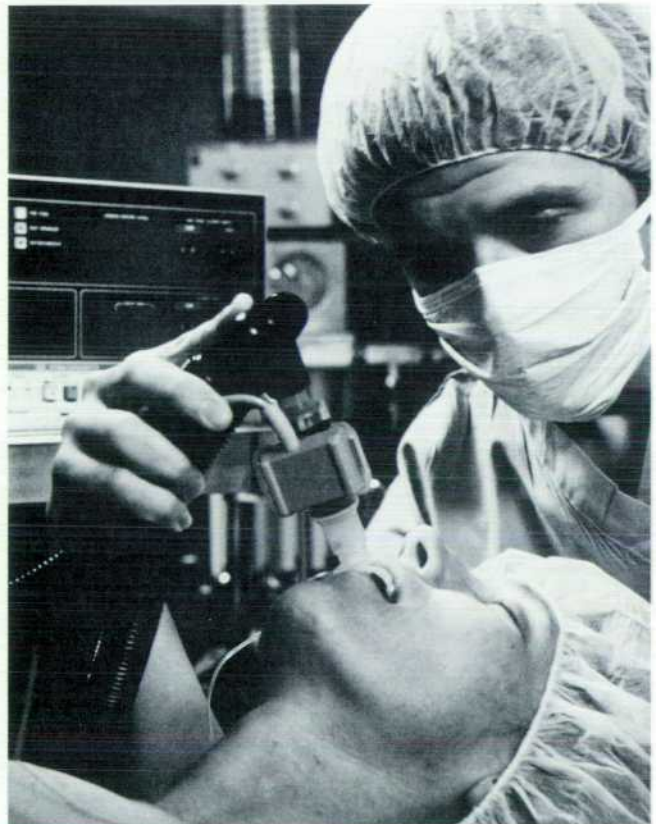


**Fig. 4.** The 47210A Capnometer is connected to the gas to be sampled for CO<sub>2</sub> content by the 14361A Airway Adapter. The adapter is inserted in series with the ventilation plumbing as shown.

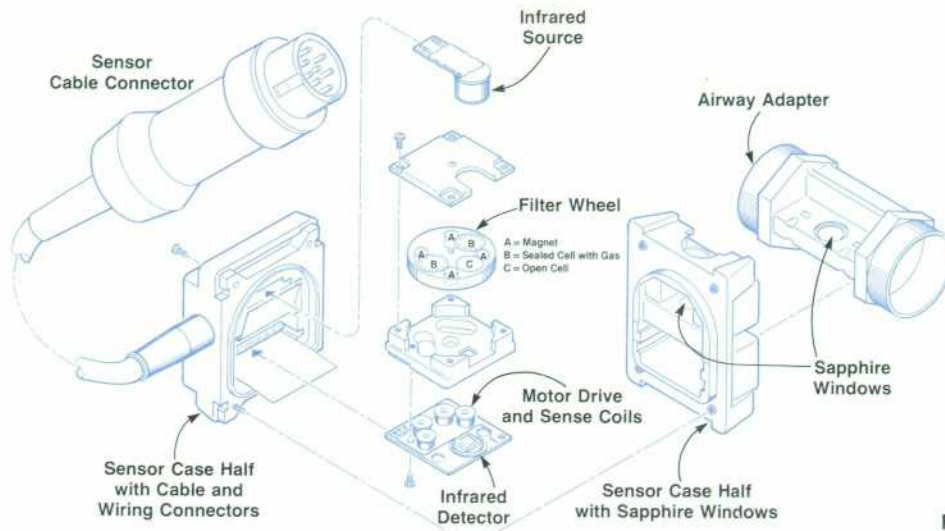


Fig. 5. Exploded view of the assembly for the 14360A Sensor.

ing is necessary if the instrument is to be beneficial in a patient monitoring situation where ease of use is given a high priority.

### Sensor Design

Starting with the lead-selenide photoresistor in the detector assembly, each part of the design interacts with the other parts. No one parameter can be changed without affecting others in the system. The design begins with the sensor.

The detector assembly, located on the opposite side of the airway adapter from the source, has a rotating filter wheel, a thin-film infrared bandpass filter and a lead-selenide photoresistive detector arranged as shown in Fig. 5. The gas sample is always in the infrared path. Modulation for drift rejection is accomplished by the rotating filter wheel. The filter wheel consists of two hermetically sealed cells with sapphire windows, one open chamber with sapphire windows, and four permanent magnets. The magnets form the rotor for a brushless dc motor (see box on page 8). Each cell is rotated into the infrared energy beam 40 times per second. The output of the detector is shown in Fig. 6. The output waveform is generated as the wheel successively rotates into the infrared energy beam first one sealed cell, then the open chamber, the second sealed cell, and finally an opaque region for zero output. The conversion of this waveform to a CO<sub>2</sub> value is discussed in the box on page 12.

To obtain adequate signal-to-noise ratio so that the specified output noise of 0.5 mmHg rms can be achieved, a 3-mm-square photoresistor is used. Dark-current noise is excessive if detectors smaller than this are used. This photoresistor size defines the minimum aperture of the rotating wheel cells that can be used and still provide an adequate dwell period. This aperture controls the wheel diameter and thus the overall detector assembly size. The result is a roughly 20-mm-square by 10-mm-thick beryllium-copper investment-cast housing for the detector assembly. In addition to the filter wheel and its motor drive coils, the housing also supports two thermistors: one for temperature sensing and one for heating.

The infrared source is a heated broadband black-body radiator. The heating element is a thin-film cermet resistor

deposited on a 0.064-mm-thick sapphire substrate. Two conductors are deposited over the resistor material such that a square heater is defined in the center of the element (Fig. 7a). The heating element is mounted in a twin-lead TO-5 transistor package with a sapphire window in the top. The element is supported on the two lead posts and faces a collimating mirror mounted to the package's header (Fig. 7b).

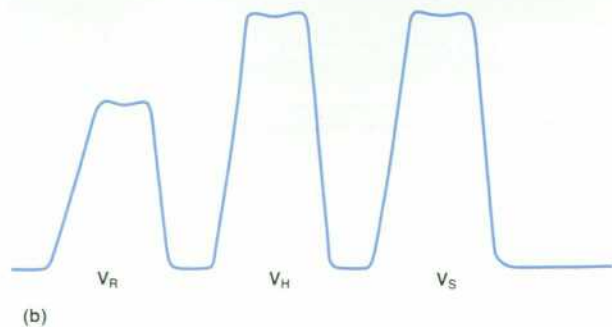
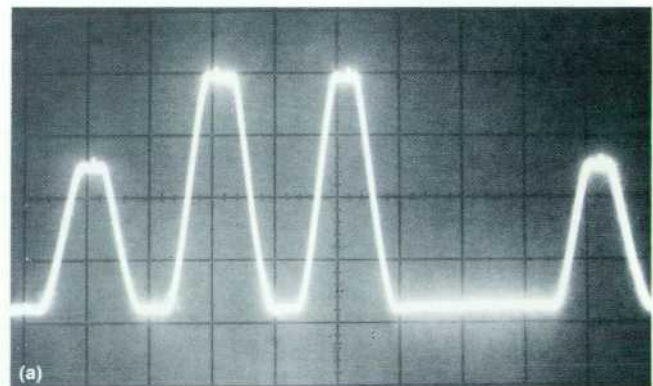
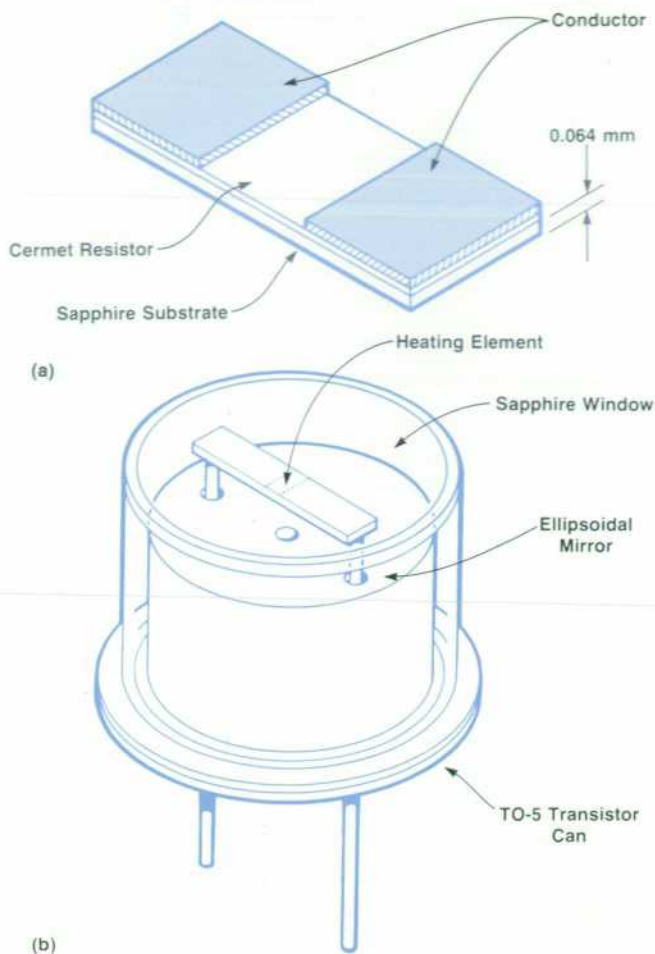


Fig. 6. (a) Typical output waveform from the infrared detector assembly. (b) Viewing the waveform from left to right, the first peak  $V_R$  is the output detected through the sealed CO<sub>2</sub> reference cell, the second peak  $V_H$  is through the open cell, and the last peak  $V_S$  is through the sealed nitrogen cell.



**Fig. 7.** (a) Cermet resistor heating element used for the infrared source. (b) Infrared source assembly. The heating element is mounted face downward so that the mirror can focus the infrared radiation.

The detector assembly and the source define the basic dimensions and weight of the sensor. What about ruggedness, cleanability and voltage isolation? The design of the outer case assembly, from the cable entrance down to the sapphire windows, is an exercise in materials selection and testing.

The case assembly consists of two halves (Fig. 5 and Fig. 8). The upper half of the assembly contains the cable and interconnects, and the lower half aligns the infrared components. An O ring makes a watertight seal between the two halves. The thermoplastic bumpers bonded to the corners of the outer case provide necessary cushioning.

The case material is a glass-filled thermoplastic polyester. This material has the solvent resistance and dielectric strength required for the application. However, its solvent resistance makes it difficult to find a suitable adhesive for potting the cable, attaching the bumpers and sealing the sapphire windows. Each application presents a different set of requirements.

For example, the bumper-to-case bond has to be flexible and still survive multiple exposures to liquid sterilizing agents. A two-part polyurethane adhesive is used. But this adhesive generates small amounts of carbon dioxide during

its very lengthy curing cycle which can continue after the sensor is in service. This makes this adhesive unusable inside the sealed sensor because the detector assembly cannot differentiate CO<sub>2</sub> in the sample chamber from any high concentrations of CO<sub>2</sub> in the infrared path that may be trapped inside the sensor.

Finding an adhesive that would adequately bond the sapphire windows to the case material involved much trial and error. The bond has to be strong and survive exposure to sterilizing materials. A heat-cured epoxy preform is used. Precision tooling and carefully controlled technique are required because any voids in the adhesive will compromise the high-voltage breakdown resistance so necessary in an instrument used near a patient who may be subject to defibrillation.

The result is a sensor that survives drops from a height of one metre onto concrete floors without damage. The sensor has been dropped from as high as 2.4 metres. Damage was confined to the outer case structure. This severely abused sensor still measured CO<sub>2</sub> with no perceptible shift in output.

### Airway Adapter

The sensor performs its job by passing infrared energy through the airway adapter and measuring the amount absorbed by any CO<sub>2</sub> in the airway. The airway adapter also has a number of critical requirements. Sterilizability, a stable infrared path length, and ruggedness dictate a series of materials requirements. Measurement accuracy is related directly to the infrared path length through the sample. Any variation from the nominal 3-mm gap results in an error proportional to the difference in the gap from the nominal value. To achieve the required stability in view of the other requirements, the airway adapter is made of aluminum. The choice of an aluminum investment casting is dictated by the detail necessary in the part. Grooves for the ball detents used to secure the sensor assembly to the airway adapter, the complex gas passageway with its mushroom-shaped cross-section, and the mating ends of the airway adapter precluded fabrication processes other than casting. Investment casting is used because the number of units and the

(continued on page 9)

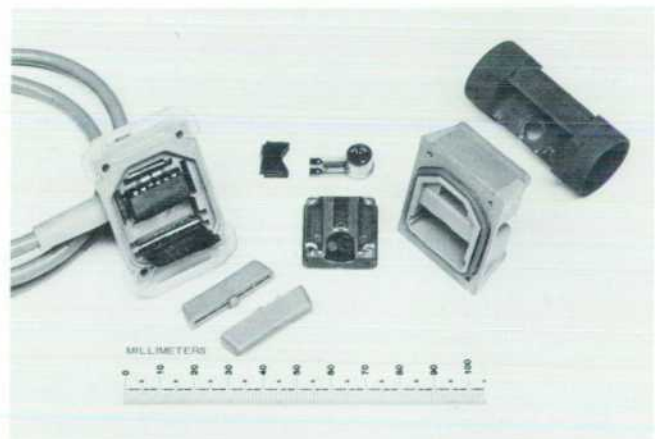


**Fig. 8.** Disassembled 14360A Sensor showing case halves (right and left), infrared source (top center), and filter wheel assembly (center).

## A Miniature Motor for the CO<sub>2</sub> Sensor (with Thanks to Kettering)

by Edwin B. Merrick

Into the midst of the tightly packed infrared components of the sensor for the 47210A Capnometer it is necessary to insert a highly reliable and efficient motor whose only purpose is to keep a little cell-carrying wheel turning at a constant rate. Among the rather stringent requirements are that the motor must not significantly increase the sensor size and cost. A sensor the size of a brick just will not do. It is also desirable to minimize the number of wires in the sensor cable, thereby keeping the cable small and light. The patient's airway tubing is already sufficiently rigid to be an encumbrance. The cable to the CO<sub>2</sub> sensor should also not add to the leverage applied to hose connections. Since the sensor

is temperature controlled at as low a temperature as possible it is necessary that the motor dissipate the least possible power. Finally, whatever motor is developed must be agreeable to accurate speed control.

Various alternative motor and drive configurations were considered and discarded. A dc brush motor? Brush noise, life and the added commutator and winding space ruled it out, although only requiring two leads was attractive. An ac induction motor? The addition of a squirrel cage or suitable conductor to the simple plastic filter wheel seemed to add size, weight or complexity when the requirements of the infrared paths were considered. Efficiency was also doubtful since the usual approach is to apply high magnetic field intensity to keep the rotor from slipping and provide speed control. A step motor approach? Now that had some promise since small permanent magnets could be added to the perimeter of the filter wheel and interspersed with the four infrared openings. This would have negligible effect on the size of the wheel. Two drive coils could be positioned away from the infrared detector on the same side of the wheel as the detector without adding to the thickness of the assembly since the detector and infrared filter already required a reasonable space (see Fig. 5 on page 6). But how should it be driven?

An optical sync track applied to the edge of the wheel as shown in Fig. 1a was tried first. This was the only wheel surface that was not otherwise occupied and could still be viewed. This track was used to drive a solid-state commutator in the processor box which then pulsed the drive coils at appropriate times in proper polarity. Initially the drive coils always received the same high pulse amplitude. This was inefficient. Thus, proportional control was applied to the pulse amplitude, applying only the drive level necessary to maintain the proper 2400 rpm. Although this motor ran, it required several wires for the optical sync signal, it increased the size of the sensor somewhat, and introduced a requirement for a second axis of optical alignment to the wheel. Also it seemed possible that efficiency might improve if just the right waveform were applied rather than an arbitrary square pulse.

(continued on next page)

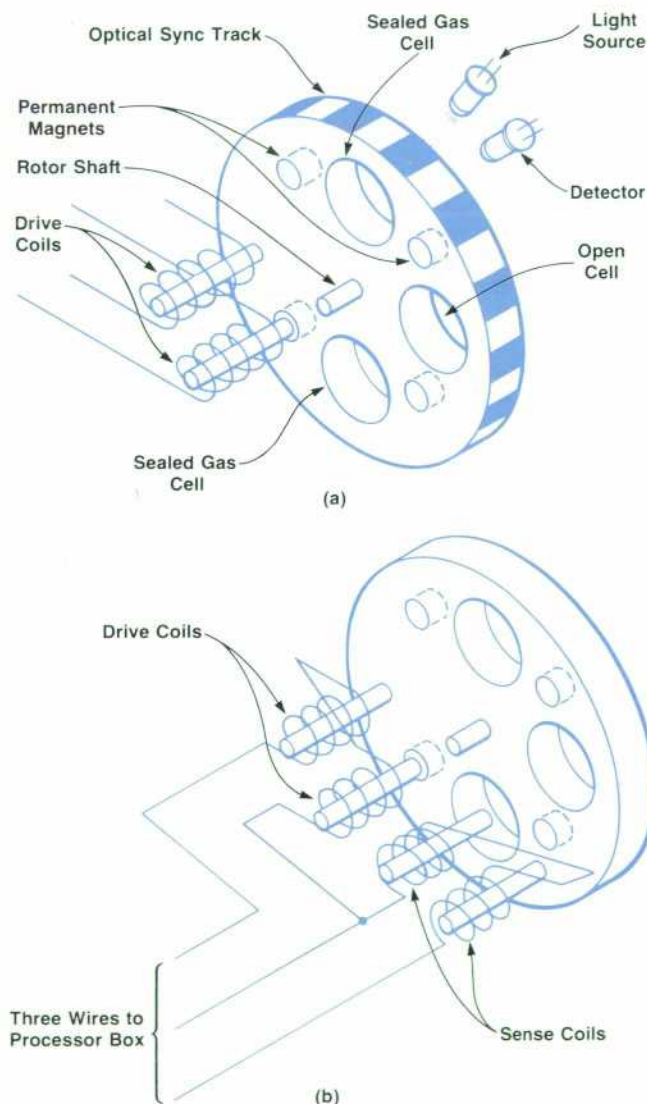


**Fig. 1.** (a) An optical sync track along the edge of the filter-wheel rotor as shown was initially used to control motor speed. (b) The sync track was eliminated in the final design by using sense coils to detect motor speed. The physical arrangement of the drive and sense coils is shown in Fig. 11a on page 11.

### Edwin B. Merrick



Ed Merrick is a native of Andover, Massachusetts and received the BSEE degree from the University of New Hampshire in 1963. He came to HP that same year and is currently an engineering manager at HP's Hospital Supplies Operations in Chelmsford, Massachusetts. Ed is co-author of an earlier HP Journal article on the 47201A Oximeter and a co-inventor on a patent for a blood perfusion measurement. He is a member of the American Association for Medical Instrumentation. Ed is married, has three children, and supports a menagerie consisting of a dog, three cats, four pigs, and a rabbit. He lives in Stow, Massachusetts where he is restoring a 200-year-old house and barn and has built a hydraulic log splitter to supply firewood for wood heating. During the summer Ed enjoys sailing his 32-foot sloop along the New England coast.

### Enter Kettering.

In describing his life's work as an inventor Kettering referred to his work on the development of a piston for diesel locomotive engines. He said the problem was not so much knowing when you had a bad piston because the engine would tell you that soon enough. The trick was to simply let the engine tell you which pistons it liked best. In this case we let the motor show us the proper drive waveform. Simply adding a pair of sense coils in the proper location and a simple integrator in the processor box produces a properly phased and shaped waveform with which to power the drive coils (see Fig. 1b). Speed control is achieved by comparing the period of the sense-coil waveform with a one-shot time reference. The speed is increased by increasing the gain of the drive amplifier and decreased by decreasing the gain.

The result is a motor that requires only three wires, uses inexpensive components, is easily speed-controlled, does not increase the size or complexity of the sensor, and runs on less than 50 mW.

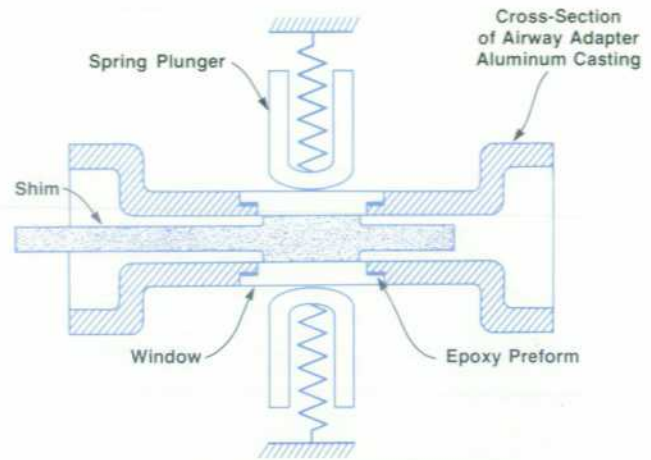


**Fig. 9.** To insure the proper gap between the two sapphire windows in the airway adapter during the curing of the epoxy adhesive they are held against a shim whose thickness is equal to the desired gap. The shim is then removed.

detail required make die casting undesirable.

The airway adapter has two sapphire windows that are epoxy bonded to each side of the gas passage. The gap between the windows forms the precise path length for the gas sample. A tolerance of  $\pm 13 \mu\text{m}$  was deemed necessary and possible. This small variation alone can add approximately  $\pm 0.4 \text{ mmHg}$  error to a 100-mmHg  $\text{PCO}_2$  measurement. The gap is set to the desired value during assembly by placing a shim of the correct thickness between the two windows (Fig. 9). By firmly clamping the windows to the shim while the epoxy bond cures, the gap is formed.

### Processor Box

The diversity of disciplines and requirements for the sensor's mechanical design is matched by the diversity of design challenges presented by the processor box, which performs the following functions:

- Sensor motor control
- Sensor temperature control

- Sensor infrared source supply
- Sensor infrared detector amplifier
- Calibration of sensor
- $\text{PCO}_2$  computation
- Altitude correction
- Interfering gas correction
- Sensor internal  $\text{PCO}_2$  correction
- End-tidal (peak) detection
- Respiration rate computation, and
- Various display and system interface tasks.

The first four functions are performed in the electrically isolated portion of the processor box. The sensor interface is isolated from chassis ground as a second line of defense against microshock hazard to the patient (the plastic sensor case being the first). A dangerous situation can occur if the sensor cable shield or internal conductors become exposed

(continued on page 11)

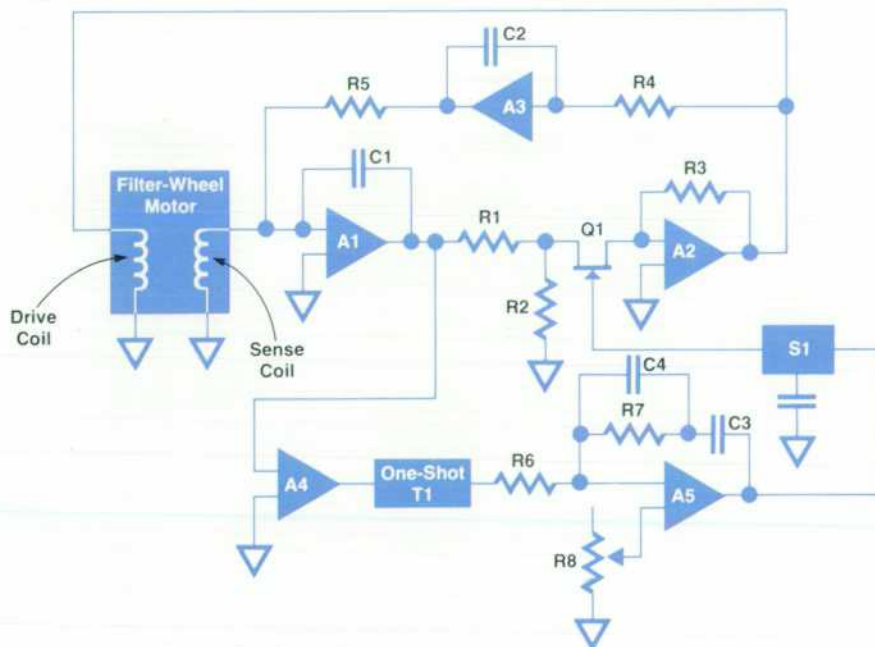


**Fig. 10.** Simplified schematic of the filter-wheel motor speed control circuit.

## Fabrication of the Sensor Requires Special Care

Because of the small size of the sensor, normal assembly techniques are difficult to use. Assembling the bearing used to support the filter wheel is an example. The constraints are to produce a low-friction, low-noise bearing that will survive the rigors of being mounted in a sensor that will be subjected to severe handling. It is extremely important to maintain the location of the wheel axially and radially. If there is too much variation in the position of the wheel as sensor orientation is changed, the output will be affected. To maintain the orientation-induced error of the sensor within acceptable levels, the radial play in the two bearings, one on each side of the wheel, is held to less than  $10\ \mu\text{m}$ . Axial play is held to less than  $50\ \mu\text{m}$ .

The normal approach for building an assembly such as this is to take the two raw castings, assemble them, and pin the two castings so that they can be disassembled and reassembled in exactly the same relative location. The bearing bores are then machined together. The castings are disassembled, the bearings inserted, the filter wheel is positioned in place and the castings are reassembled. This procedure has a number of drawbacks. First, there is insufficient room for pins. Second, because of the inherent lack of flatness and uniformity of the castings, reassembling the castings so that the bores will still be in line cannot be assured. Also, for the above technique to work, the bearing's outside and inside diameters must be held to tolerances tight enough that the bores in the bearings will line up when the casting holes do. This is not possible when sintered bronze bushings are used. Sintered bronze bushings were selected instead of ball bearings for the sensor because they are more rugged and quieter.

The solution is to mount the unrolled bushings in the castings with a modified acrylic anaerobic adhesive. No pins are used to align the two castings. The assembly process requires two separate fixtures that are illustrated in Fig. 1. The first takes the two casting pieces, with the wheel and shaft captive in the bearing bore, and aligns the bearing bores. The bearings are not yet in place. The four screws holding the castings together are then tightened. The second fixture is used to install the two bearings in the castings on either side of the filter wheel. This fixture holds the wheel, bearings, and casting so that the correct axial play is maintained and the bearings are aligned, but the radial clearance between the shaft and the bearing is not reduced.

The problem that must be addressed is that the shaft may be bowed slightly; thus the filter wheel may not turn freely throughout its full 360 degrees of rotation. By allowing the bearings in the castings to be self-aligning with respect to the shaft and biasing the wheel and shaft to one side with a specified side load during the adhesive curing cycle, the radial clearance is established and alignment between the shaft and bearings is assured. The shaft and bearings are supported by spring-loaded pins. By pressing the bronze bearings firmly against the two jeweled ringstone thrust bearings on the filter wheel and elastically deforming and holding the casting during the cure cycle the proper end play is established when the casting returns to its unstressed state upon removal from the fixture.

Other portions of the sensor are designed to use fixturing as an integral part of the manufacturing process. Fixtures are used to locate the infrared detector and the four motor coils on the printed circuit board during assembly. The upper and lower case assembly technique also uses fixtures to align components such as the sapphire windows during the bonding phase.

The sensor requires two stable gas mixtures, each hermetically

sealed in a transparent cell for use in the filter wheel. One cell has to contain an accurately determined, stable reference concentration of  $\text{CO}_2$ , the other has to contain only nitrogen. The fabrication problem is two-fold. The first is how to construct the cell such that acceptable hermeticity can be maintained, and the second is how to fill and then seal the cell with an accurately determined concentration of  $\text{CO}_2$  inside. The approach chosen bonds a sapphire window to each end of a metal cylinder. After a number of trials, the window-to-ring bonding method selected is a glass frit seal to a Kovar™ metal ring. Other methods such as epoxy adhesives or brazing operations were either too permeable, thus allowing the gas concentration to change, or too expensive.

(continued on next page)

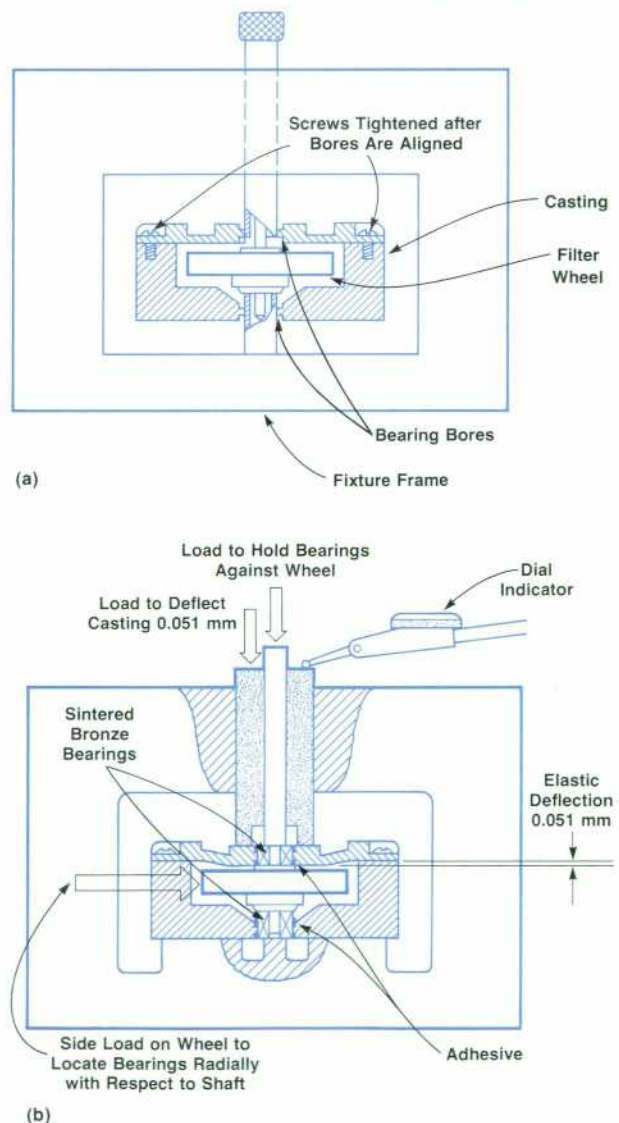


**Fig. 1.** (a) This fixture design aligns the bearing bores in the detector assembly before the four screws holding the assembly together are tightened. (b) This fixture design aligns and loads the filter wheel shaft and bearings in the detector case assembly while the adhesive securing the bearings cures.

Filling the cell and then sealing it is the next challenge. Using a filling tube brazed to the metal ring and closed by crimping was cumbersome and expensive. A radial hole located directly in the wall of the ring is the approach used. The filling and sealing process is done by inserting a solder preform loosely in the hole and then placing many filter cells in a sealing vessel. The sealing vessel is first evacuated and baked to remove residual gas contamination. Next, the vessel is backfilled with the appropriate CO<sub>2</sub> concentration and sealed. The temperature is then elevated past the solder melting point. The solder flows, sealing the hole. The vessel is then allowed to cool slowly. The cells are removed from the vessel and measured to assure that the CO<sub>2</sub> concentration contained in each cell is within acceptable limits before they are mounted in the filter wheel.

and the patient contacts the exposed wires. If at the same time the patient contacts a current source such as a defective, electrically operated hospital bed, this second line of defense prevents more than 100 microamperes of current from flowing through the patient to earth ground via the sensor.

Accurate speed control and good dynamic response are necessary for the control of a somewhat unusual motor (see box on page 8). Because the infrared beam is modulated by the rotating filter wheel, it is necessary to sample the infrared signal at just the right time.

The periods when the infrared signal rises and falls are contaminated with light rays that have experienced multiple reflections from the sidewalls and edges of the many infrared components. This situation results in an error of up to one mmHg of PCO<sub>2</sub> for each 50  $\mu$ s of sampling time change. In addition, 50 and 60-Hz power-line fields can add to the signal noise if the sampling rate of the infrared signals is not controlled. The importance of the dynamic response of the speed control will be appreciated if it is remembered that the patient's respiratory efforts impart motion to the ventilator plumbing and thus the sensor. This motion can momentarily rotate the sensor housing slightly with respect to the filter wheel, causing an apparent change in its rotational velocity.

The circuit diagram in Fig. 10 shows the motor speed control. Amplifier A1 and capacitor C1 form an integrator whose output is proportional to the flux change in the sense coils produced by the four moving magnets on the motor's rotor (the filter wheel). Note that the output amplitude is not a function of rotational velocity. Resistors R1 and R2 form an attenuator which provides a low-level signal to Q1, a FET used as a controlled-resistor element. Amplifier A2 supplies the motor drive coils. Amplifier A3 and capacitor C2, also connected as an integrator, are responsible for keeping the dc output of A2 at zero volts. Four times each revolution a zero crossing of magnetic flux is detected by comparator A4, which then triggers T1. The average value of T1's output is compared to a reference voltage set by R8. Any difference between these two voltages is integrated by A5 and, through a sample-and-hold circuit S1, the result is applied to the gate of Q1. Thus, if T1 is triggered too often (indicating a high speed) the gate of Q1 will be adjusted in a negative direction, thereby reducing the drive applied to the motor. Network C4-R7 compensates for the inertia of the motor's rotor.

The temperature of the detector assembly is another critical parameter that must be controlled accurately. Of all the infrared elements, the interference filter is the most sensitive. Small changes in temperature cause the filter's center wavelength to change sufficiently to alter the CO<sub>2</sub> measurement. A straightforward thermistor-amplifier-heater circuit, heavily compensated for thermal lag, is used.

One feature of the temperature control is the placement of the temperature sensor (a thermistor) and the heater relative to the infrared filter (see Fig. 11). In a typical analog heater control, variable gradients occur between the heated area and the thermistor in response to thermal load. As heat is removed from the system, the thermistor will cool below a desired temperature and the heater will be turned on. Because the system has finite gain, the area near the heater will get much warmer due to the increased heat input while the thermistor is still cooling. In this particular case, with the filter between the thermistor and the heater, a system gain is chosen so that temperature changes at the filter are minimal, providing the filter with optimal temperature control and therefore minimizing the temperature sensitivity of the sensor.

(continued on page 13)

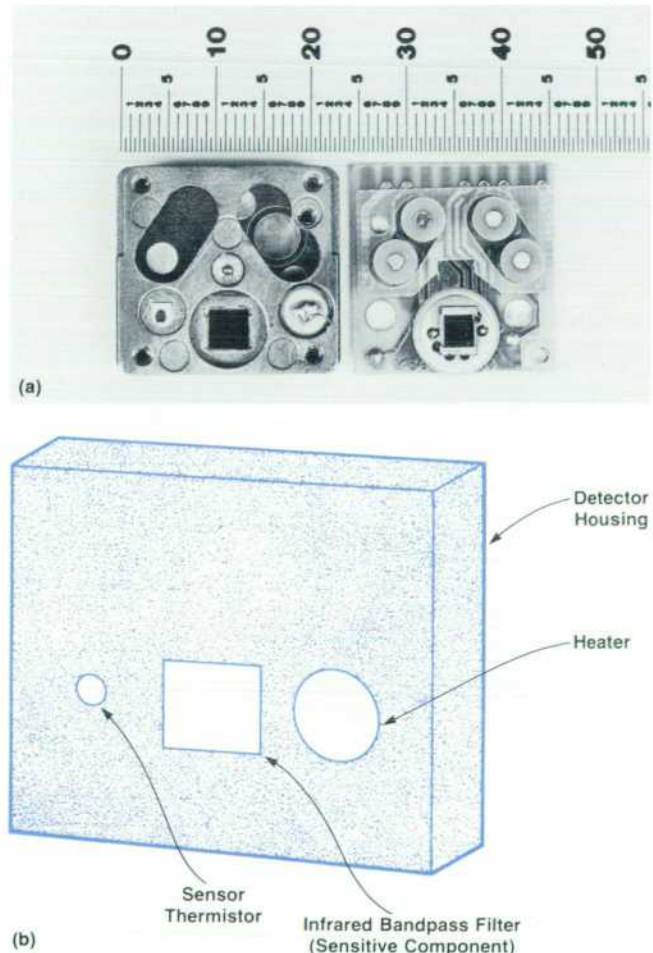


Fig. 11. (a) Photograph of the infrared detector assembly showing the filter wheel and infrared filter on the left and the printed circuit board with the motor coils and infrared detector on the right. (b) Infrared filter temperature variations are minimized by locating the thermistor and heater for the filter's temperature control on opposite sides of the filter as shown.

# An End-Tidal/Respiration-Rate Algorithm

by John J. Krieger

One of the features of the 47210A Capnometer, when used with an airway adapter, is the generation of derived parameters: respiration rate, end-tidal  $\text{PCO}_2$ , and inspiratory minimum  $\text{PCO}_2$ . The main purpose of the capnometer is to measure a carbon-dioxide partial-pressure waveform accurately and precisely. The waveform itself is useful for diagnostic purposes, but most capnometer users are interested in the parameters derived from the  $\text{PCO}_2$  waveform. In the 47210A the microprocessor controlling the capnometer also analyzes the  $\text{PCO}_2$  waveform and derives these desired parameters.

Simply speaking, an airway  $\text{PCO}_2$  waveform looks like a distorted square wave (see Fig. 1). The waveform increases to a peak value at the end of each breath cycle; this is called the end-tidal ( $\text{ETCO}_2$ ) value. In patients that do not have chronic obstructive lung disease, the  $\text{ETCO}_2$  value very closely approximates the  $\text{PCO}_2$  level in the arterial blood.

Some  $\text{CO}_2$  analyzers on the market attempt to derive an  $\text{ETCO}_2$  value from a  $\text{PCO}_2$  waveform by using analog circuitry and performing a simple peak-finding function. This may work fine for normal waveforms, but most real  $\text{PCO}_2$  waveforms contain noise and waveform artifacts caused by the patient coughing or moving (or crying in the case of children) or by ventilator waveform distortion. For example, amplitude variations can be caused by intermittent mandatory ventilation (IMV). IMV is used where patients usually can breathe on their own, but occasionally need help by forced ventilator breathing. Under these conditions a simple, analog peak-finder does not perform very well in deriving accurate  $\text{ETCO}_2$  values.

To develop the end-tidal/respiration-rate algorithm for the 47210A Capnometer, many field trials were performed at several hospitals internationally. At these trials,  $\text{PCO}_2$  waveforms were recorded on magnetic tape from many patients with a variety of diseases and a variety of ventilators—including operating room ventilators. The dozens of hours of recordings were digitized and stored on a computer disc file for easy random access. An algorithm development system was programmed on an HP Model 9845B Desktop Computer with CRT graphics. A proposed end-tidal algorithm was entered into the 9845B. Then, a variety of real patient  $\text{PCO}_2$  waveforms was retrieved from the disc file to test the proposed algorithm. The waveform and the derived parameters were displayed on the CRT screen. The algorithm was then evaluated for effectiveness and modified to achieve best performance. Once the optimum algorithm was achieved, it was coded into microprocessor assembly language for use in the 47210A Capnometer.

The end-tidal/respiration-rate algorithm has several requirements. Not only does it have to find the minimum and maximum  $\text{PCO}_2$  and the period between breaths, but it also must recover from all possible error conditions. The error conditions may be caused by a variety of sources: initial instrument warmup transients, pseudo- $\text{CO}_2$  waveform glitches caused by electromagnetic interference (EMI) from electrosurgery devices, changing the  $\text{CO}_2$  sensor from one patient to another, patient breathing artifacts (coughing, crying, sighing, long periods between breaths, or resisting the ventilator), and ventilator artifacts caused by poppet valves, tubing elasticity, trapped water, pulsation, et cetera. Normal people have  $\text{ETCO}_2$  values of about 40 mmHg. Patients with chronic obstructive lung disease may have  $\text{ETCO}_2$  values in excess of 90 mmHg!

The problem of extracting the  $\text{ETCO}_2$  from a patient on a ventilator under intermittent mandatory ventilation proved to be difficult. In that situation, the question becomes "which waveform peak is the  $\text{ETCO}_2$ ?" An IMV  $\text{PCO}_2$  waveform ensemble contains several  $\text{ETCO}_2$  peaks of varying amplitude. The forced ventilation breath usually produces the largest  $\text{ETCO}_2$  value and the several intermediate and weaker voluntary breaths produce  $\text{ETCO}_2$  values of decreasing amplitude. This is probably because the forced breath is effective and the shallow, voluntary breath is less effective and represents the rebreathing of a larger fraction of tubing dead-space. In the transition stages when a patient on IMV is getting stronger, the patient's voluntary breath  $\text{ETCO}_2$  values are about the same as the forced breath  $\text{ETCO}_2$  values.

Sometimes the  $\text{PCO}_2$  waveform is meaningless and no reasonable  $\text{ETCO}_2$  or respiration-rate derivation can or should be made. In this case, an error message is displayed on the 47210A front panel to indicate something is wrong with the quality of the data. This can alert the nurse or physician that a patient or ventilator problem exists.

The final algorithm has some resemblance to its analog predecessors in that it is the digital equivalent of a low-pass filter. A low-pass-filtered waveform is used as an adaptive threshold for determining when a maximum (end-tidal) or minimum (inspiratory minimum)  $\text{PCO}_2$  value has occurred. The digital algorithm then makes waveform feature decisions based on time window criteria. The time windows are also adaptive and are updated based on the patient's past breathing history. This type of filtering in both the time and frequency domains is very difficult to do with pure analog circuitry.

Actually, two low-pass-filtered threshold values are computed. The mean  $\text{PCO}_2$  value is the low-pass-filtered result of the instantaneous  $\text{PCO}_2$  waveform and has a time constant of about 60 seconds. The peak-to-peak index is a measure of the deviations of the instantaneous  $\text{PCO}_2$  waveform from the mean  $\text{PCO}_2$  value. This second value is analogous to the amount of ripple in the output of a full-wave rectifier circuit and also has a time constant of about 60 seconds. The peak-to-peak index is scaled down and

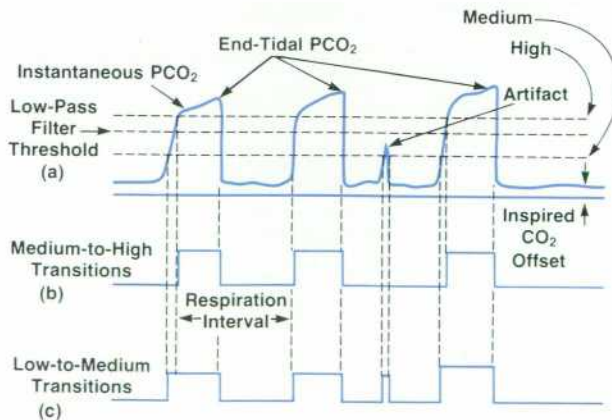


Fig. 1. (a) Partial-pressure  $\text{CO}_2$  waveform. Each pulse corresponds to one breath by the patient. The capnometer software algorithm derives the medium-to-high (b) and low-to-medium (c) waveforms to determine respiration rate and eliminate artifacts.

used to create a hysteresis band about the mean  $\text{PCO}_2$  value. Two threshold levels are derived as follows:

$$\begin{aligned} \text{Threshold (HI)} &= \text{mean} + (\text{peak-to-peak index})/4 \\ \text{Threshold (MED)} &= \text{mean} - (\text{peak-to-peak index})/4 \end{aligned}$$

The instantaneous waveform is divided into three sections: low, medium, and high (see Fig. 1). By counting the transitions from one region to another, the basic breath cycles can be determined. The time interval required to complete a cycle (low-medium-high-medium-low-medium) determines the respiration interval.

Using the three-section approach helps reduce false end-tidal values caused by artifacts of a patient resisting a ventilator adjusted for intermittent positive pressure ventilation (IPPV), IMV, or other causes. A window of minimum time in the high and low regions is computed from the respiration rate. Transitions that occur in less than the minimum window time are defined as undesirable artifacts in the  $\text{PCO}_2$  waveform. Detection of such a result is displayed by an error message on the front panel. This error condition is cleared as soon as a good, artifact-free waveform is detected.

Once the  $\text{PCO}_2$  waveform is judged to be in the high region, the end-tidal value is selected to be the highest quick-average value within that region before the  $\text{PCO}_2$  value drops to the medium or low regions. This quick-averaging width is proportional to the time window, which is computed from the respiration-rate information.

The determination of the inspiratory minimum value is identical to that for determining the end-tidal value except that the point of interest, of course, is the minimum value in the low region just

before the  $\text{PCO}_2$  value changes to the medium region.

Some averaging of breath intervals is done to obtain a less erratic respiration-rate display. Moving averaging is done on the last six breath-to-breath intervals. All six breaths are equally weighted. After an apnea (that is, no breath cycles for more than 30 seconds), a break in breathing is detected and an alarm is initiated. When breathing resumes, the algorithm accumulates good breaths as they come in and averages those accumulated until there are six new values and then the algorithm resumes normal averaging.

#### John J. Krieger



John Krieger is a native of Santa Monica, California and attended the University of California at Los Angeles (UCLA) where he received the BSEE and MSEE degrees in electronics and biomedical engineering in 1974. John then joined HP and was a development engineer for the 47210A Capnometer. He recently left HP and now lives in Goleta, California with his wife and daughter. John is a member of the Society of Motion Picture and Television Engineers and enjoys scuba diving, skiing, Chinese cooking, and photography.

Since the relative magnitudes of the alternating infrared signals are compared by the digital processing that follows, it is not important to maintain a constant infrared source output. A simple dropping-resistor scheme adequately controls the power delivered to the source element. With the dropping resistor equal to the nominal infrared source resistance, changes of 2 to 1 in source resistance caused by component variation and aging produce only an 11% change in source power. This is more than adequate to maintain sufficient signal-to-noise ratio and source lifetime.

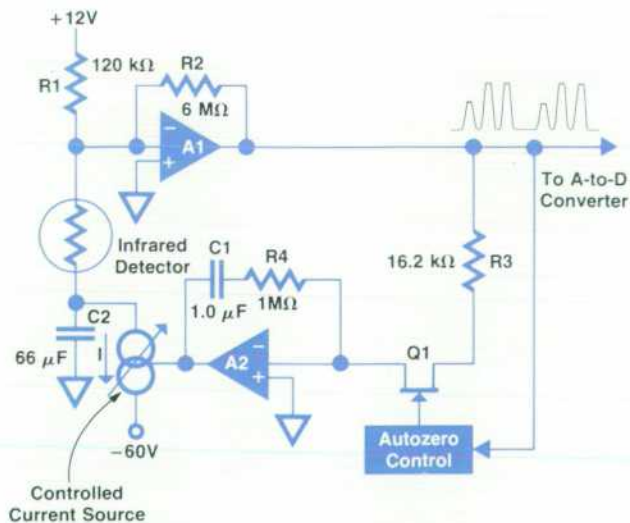


Fig. 12. Biasing and amplification circuit for the infrared detector.

The infrared detector used in the sensor is a lead-selenide photoconductor with a nominal dark resistance of 400 k $\Omega$ . This resistance varies about  $\pm 50\%$  from device to device. However, the infrared energy reaching this detector causes only about 0.15% change in its resistance. Since this change in resistance must be resolved to at least 12-bit precision, it is apparent that quiet, accurate bias and amplifier circuits are required. Fig. 12 shows a circuit diagram of how these requirements are met.

Resistor R1 supplies 100  $\mu\text{A}$  to the summing junction of amplifier A1. Under dark conditions (no incident infrared radiation), the bias voltage applied to one end of the detector is adjusted to remove the 100  $\mu\text{A}$  supplied by R1. Any change in the detector current flows through R2, provided of course that A1 has enough gain to keep its summing junction at zero volts. Since infrared energy causes a decrease of the detector's resistance, A1's output is positive-going for increasing infrared intensity. Once each filter wheel revolution, an autozero control circuit causes FET switch Q1 to close for 600  $\mu\text{s}$ . Any output voltage from A1 causes a current in R3 which, via feedback around A2, is forced to flow in capacitor C1. Therefore, after each revolution the charge on C1 is updated to cancel the error seen in A1's output. A2's output is applied to the control input of a current generator I which is adjusted each wheel revolution to make the detector current approach the current in R1. Capacitor C2 has two important functions. First, it filters out any noise produced by the active current source I. Second, C2 appears to the detector to be a voltage source during the short time required for one wheel revolution. Thus all of the small-signal detection-current changes flow into A1's summing node.

With the five functions of motor control, temperature

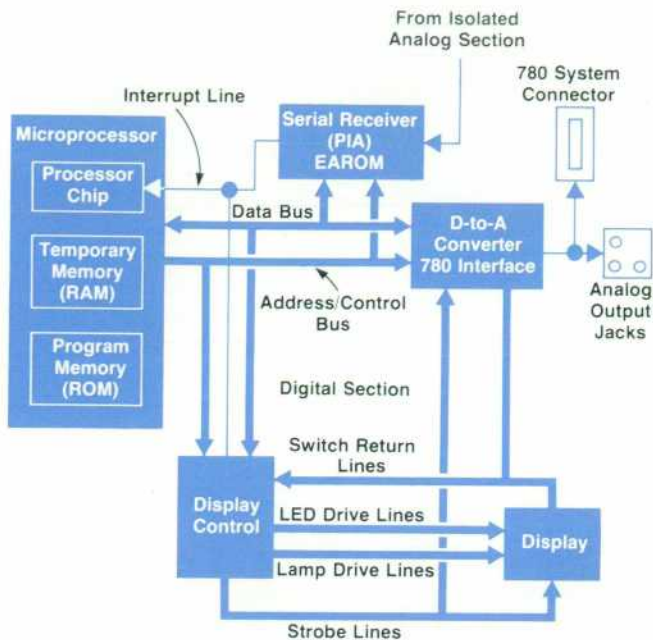


Fig. 13. Block diagram of the digital electronics section in the processor box of the 47210A.

control, source power control, detector bias and amplification accomplished, the sensor output is suitable for conversion to digital form for further processing. The sensor's analog output waveform is prescaled by one of four possible gains in a preamplifier. The gain switching is done via control from the microprocessor and allows the analog-to-digital (A-to-D) converter to function as a fixed-point 14-bit A-to-D converter, thus minimizing unused bits. This prescaled waveform is converted to four sampled values corresponding to the three filter-wheel-cell readings plus one dark reading. The triple-slope A-to-D converter is triggered to sample the appropriate 248- $\mu$ s-wide pulse of the infrared output waveform by the motor sense-coil signal. The four 14-bit words are transmitted serially to the grounded electronics portion of the processor box by an optical coupler (Fig 2).

### Digital Processing

The 47210A Capnometer's processor box contains microprocessor electronics to perform all the magic needed to convert the stream of digital data from the sensor to meaningful physiological data. The digital electronics (Fig. 13) consists of a microprocessor, volatile random-access memory (RAM), 12K bytes of program read-only-memory (ROM), a nonvolatile electrically alterable ROM (EAROM), input logic, and logic to output information to the user. The output information consists of front-panel numeric displays for CO<sub>2</sub> and respiration rate parameters, front-panel light-emitting-diode (LED) annunciators such as alarm lights, rear-panel analog outputs driven by a digital-to-analog (D-to-A) converter, and other rear-panel output signals which are used when the capnometer is connected to an arrangement of other bedside monitors.

The microprocessor (MPU) receives command sequence information from the program ROM. The MPU activates its

various system components to perform several tasks necessary to convert the digital data into PCO<sub>2</sub> and other derived parameters. A main program (see Fig. 14) performs most of the major tasks.

When electrical power is first turned on, each of the MPU system components is tested for functionality. A checksum test is performed on each of the three program ROMs. If a ROM fails this test, a message indicating its printed circuit board location is displayed on the capnometer's front panel. The volatile RAMs are tested by a checkerboard RAM test pattern. The EAROM, the programmable interface adapter (PIA), and the keyboard/display scanner devices are also tested by appropriate algorithms. Again, if any device fails its test, its printed circuit board location is shown on the display. If nothing is defective, the main program continues by initializing all the RAM data structures and I/O devices. The main program then awaits the data-available signal flag before continuing.

This wait loop can be interrupted by hardware when a high-priority, real-time event (such as when an A-to-D conversion is completed) needs attention. When an I/O device (such as an A-to-D converter) requests service, the main program is stopped and its state is stored so that it can be restarted later when the cause of the interrupt has been serviced. The MPU then vectors to an interrupt service routine that identifies the source of the interrupt and performs the appropriate action. The interrupt may be due to one of several causes (see Fig. 15).

The non-maskable interrupt (NMI) is reserved for instrument servicing. In this case, a test loop generates a stable, synchronous digital pattern needed for digital signature analysis testing. This makes it possible to test field failures down to the component level.

The maskable interrupt (IRQ) can be activated by the A-to-D converter, the 100-Hz real-time clock, or the keyboard/display scanner chip. When the IRQ is activated, its service routine polls the I/O devices to determine the cause of the interrupt and then the appropriate I/O device is

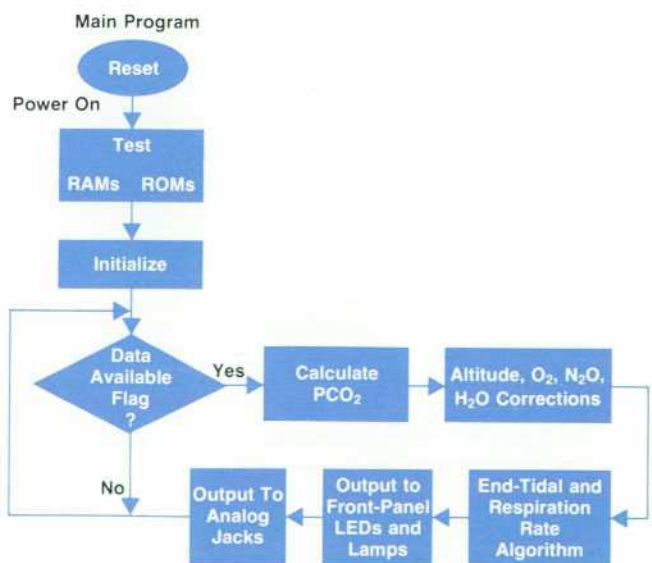


Fig. 14. Flow chart of the main control program for the capnometer.

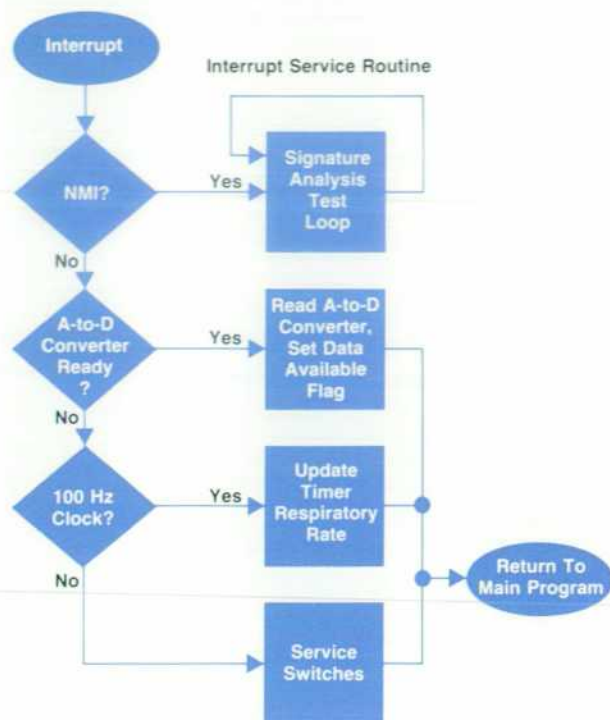


Fig. 15. Flow chart of the subroutine used to determine the source of an interrupt.

serviced. If the A-to-D converter is the cause, a digital value and status bits are collected. The data-available flag is set by the A-to-D service routine only when all the elements of the A-to-D message have been collected from four revolutions of the transducer's filter wheel. The real-time clock interrupt is used for time-related computations, such as converting a CO<sub>2</sub> waveform breath-to-breath interval to respiration rate (breaths per minute). The keyboard/display scanner chip triggers an interrupt whenever a front-panel switch is pressed. This is important because the user may wish to change the operational state of the capnometer and a switch interrupt avoids the need to poll all switches constantly.

When the main program receives the data-available signal, it processes the packet of digital data. This data, along with transducer calibration information previously stored in the EAROM, is transformed into partial pressure of CO<sub>2</sub>. This is made possible by a series of mathematical functions that include multiply, divide, square root, and exponentiation.

The basic CO<sub>2</sub> calculation described in the box on page 12 is only the next step leading to the PCO<sub>2</sub> and respiration rate display. After the PCO<sub>2</sub> is calculated, corrections must be applied to compensate for the various interfering parameters.

As was mentioned earlier, the sensor is influenced by effects other than just the partial pressure of CO<sub>2</sub> in the sample. Total pressure (altitude) as well as the presence of gases such as oxygen, water vapor, and nitrous oxide also affect the amount of infrared absorption. The effect of altitude was determined empirically on the static station described in the box on page 19. This was done by measuring the sensor output for different total pressures while maintaining a constant partial pressure of CO<sub>2</sub>. The static station was also used to measure the effect of interfering gases (see

box on page 16). Algorithms that perform the compensation routines for these errors are incorporated into the processor box firmware.

### Altitude Correction

The total pressure effect on the measurement is handled by the instrument and does not burden the operator during use. The instrument is programmed to compensate for the line-broadening effect on the measurement caused by differences in total gas pressure. At elevations other than sea level, the instrument will remain calibrated when properly set via internal rotary switches.

It is desirable to enter altitude instead of average total pressure for instrument calibration. This makes the initial instrument setup easier. The equation relating total pressure to elevation is

$$\text{BAR PRESS} = 760 \exp \left( \frac{-3.394x}{282 - 0.492x} \right)$$

where BAR PRESS is the average barometric pressure in mmHg and x is altitude in hectometres. A lookup table is used to store fourteen constants relating sensor error to the PCO<sub>2</sub> measured at each of the 50 possible altitude settings (0 thru 49 hectometres). When an altitude setting is entered, the 14 corresponding constants are used to generate a piecewise-linear approximation of the appropriate correction curve. A linear interpolation is done between adjacent points every 100 ms (at each PCO<sub>2</sub> calculation) and a correction constant (ALTK) is determined. The actual PCO<sub>2</sub> is calculated from the following relationship:

$$\text{PCO}_2 |_{\text{actual}} = \frac{1}{(1 - \text{ALTK})} \text{PCO}_2 |_{\text{measured}}$$

### Interfering Gas Compensation

The final correction applied to the PCO<sub>2</sub> computation compensates for the errors caused by interfering gases (see box on page 16). Since the instrument is calibrated on a binary carbon dioxide and nitrogen mixture, the question is how to allow the operator to reduce the effect of the interference to acceptable limits and not compromise ease of use. It seems appropriate to allow the microprocessor to perform the correction computation, so the problem becomes one of simplifying the data entry. Three assumptions were made:

1. The expired gas is saturated with water vapor at 33°C.
2. The expired oxygen partial pressure (PO<sub>2</sub>) is related to the inspired pressure by the following:

$$\text{PO}_2 |_{\text{expired}} = \text{PO}_2 |_{\text{inspired}} - \frac{\text{PCO}_2}{0.8}$$

and the minimum inspired PO<sub>2</sub> is 21%.

3. When nitrous oxide is used, it is administered in a binary mixture with oxygen in concentrations from 0% to 65%.

Three pushbutton switches on the front panel are used to implement the nitrous oxide and oxygen corrections. The first is for nitrous oxide compensation, the second is for oxygen concentrations between 21% and 50%, and the third pushbutton is for oxygen concentrations greater than 50%

(continued on page 18)

# In-Service CO<sub>2</sub> Sensor Calibration

by Russell A. Parker and Rodney J. Solomon

The success of the 47210A Capnometer is very much dependent on the ease of use of the 14360A Sensor. The ideal situation is achieved with a completely interchangeable sensor. However, because of differences in interference filters, zero and reference cell gas filling, infrared alignment and some other variables, each sensor, when used with a different 47210A, must be calibrated against a gas standard to achieve the desired measurement accuracy. This standard is the gas-cell calibration stick. Its validity is based on a major assumption that, within limits, all sensors will look alike to the processing algorithm in the 47210A after calibration on the zero and 55 mmHg gas cells. The detector signal must therefore be processed in such a way as to generate a standard response curve, the values of which relate in some known way to the partial pressure of carbon dioxide (PCO<sub>2</sub>).

The infrared system requires that the signal always pass through the sample. To avoid errors caused by source and detector output changes, signal path blockage, etc., the detector's output (VR) while a reference gas cell filled with approximately 160 mmHg of CO<sub>2</sub> is in series with the sample is compared to the detector's output (VS) when a zero cell containing no CO<sub>2</sub> is in series with the sample. These cells are part of the filter wheel assembly in the sensor. The ratio VR:VS is called Q. As CO<sub>2</sub> gas fills the sample volume, VS decreases more rapidly than VR. Q, therefore, increases (Fig. 1).

The capnometer sensor uses an infrared bandpass filter in series with the infrared beam. The passband of this filter is of sufficient width to allow the energy not absorbed by many of the discrete lines of the infrared absorption band to pass through to the detector (see box on page 4). At the concentrations of interest and given the sample path length, the relationship between Q and PCO<sub>2</sub> will not be a simple exponential as is described by Beer's Law.\* If Beer's Law held, Q would be constant regardless of the sample concentration, and the series path scheme used in the capnometer would not work.

The task then is to find an expression for Q versus PCO<sub>2</sub> which, when calibrated at only two points, will still represent the response for any given sensor within allowable tolerances. To accumulate the needed data, special sensors were designed and built to allow rapid changing of each infrared component. A matrix of experiments was performed on the static station (see box on page 19) with infrared components at tolerance extremes. After a number of trials, the form of the equation used to relate Q to PCO<sub>2</sub> is:

$$S = \frac{(Q-D)^E - (Q_0-D)^E}{(Q_{55}-D)^E - (Q_0-D)^E}$$

where PCO<sub>2</sub> is a function of S. This function is a second-degree polynomial where Q is the Q at a given PCO<sub>2</sub> from the data set, E is a variable incremented by 0.5 from 0.5 to 4.5, Q<sub>0</sub> and Q<sub>55</sub> are the sensor Q values at 0 and 55 mmHg CO<sub>2</sub>, and D is found from the following equation:

$$D = AQ_0 + BQ_{55} + C$$

where A, B, and C are variables derived by a curve-fitting routine. D is a modifier of Q that attempts to remove some of the

\*Beer's Law states that the absorption of light by a solution changes exponentially with the concentration of the solution if no other factors change at the same time.

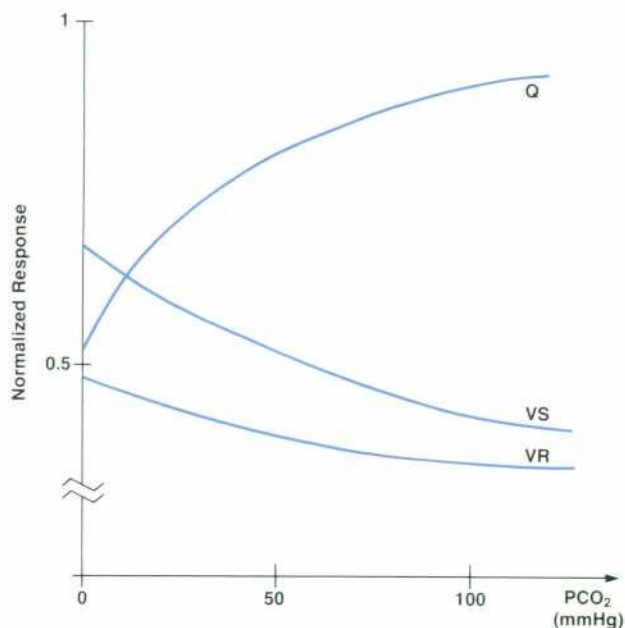


Fig. 1. The relative amplitudes of the VR and VS portions of the infrared detector output waveform (Fig. 6 on page 6) vary with PCO<sub>2</sub> level as shown.  $Q = VR/VS$ .

differences between sensor responses by compensating for the actual Q<sub>0</sub> and Q<sub>55</sub> values.

A general multiparameter least-squares curve-fitting routine<sup>1</sup> was used to relate S to Q. The goal was not to linearize S, but rather to minimize the differences between various sensors for S versus PCO<sub>2</sub> (see Fig. 2). The routine was allowed to determine the coefficients A, B and C for optimum similarity of S at each value of E used. Weighting factors were employed to force curve S to

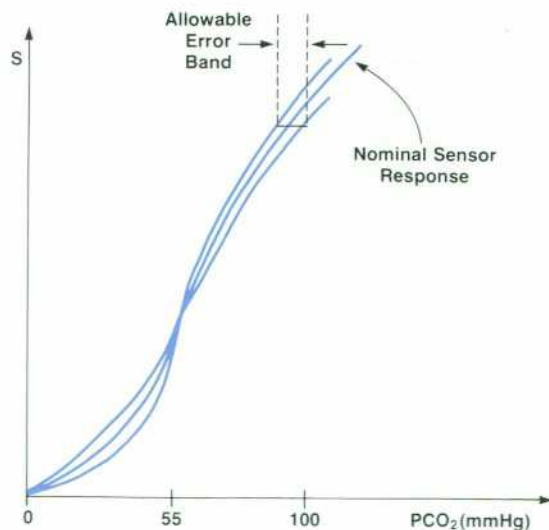
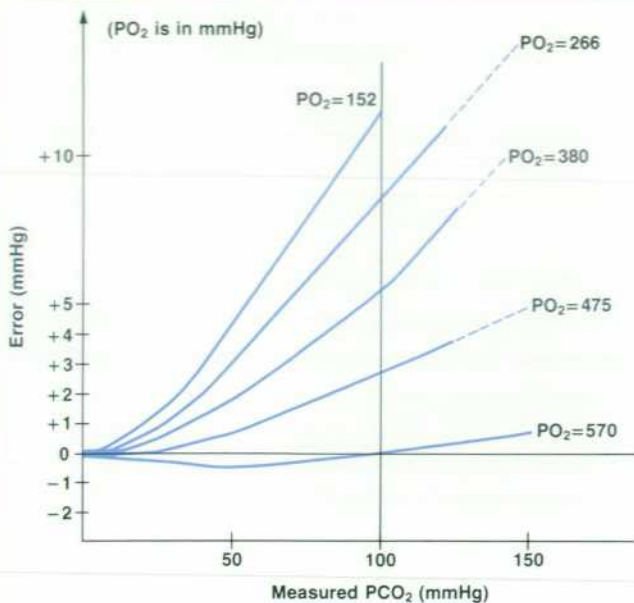


Fig. 2. Plots of S versus PCO<sub>2</sub> level for various sensors.



**Fig. 3.** Plots of the error in the uncompensated  $PCO_2$  value caused by the presence of various nitrous oxide and oxygen concentrations.  $PO_2$  is the inspired  $O_2$  pressure in mmHg and the balance of the gas mixture is  $N_2O$  for each curve.

remain in a region where, essentially, the data has the greatest slope between points. One unacceptable solution to coefficients A, B, C and E forces S to be zero at all points. Similar for all sensors yes, but this value of S can hardly be configured by a second-degree polynomial to yield  $PCO_2$ . A further constraint is that  $CO_2$  can be generated inside the sensor for a variety of reasons. Therefore, the data for all sensors was shifted to simulate 5, 10, and 15 mmHg of internal  $CO_2$ .

The result is that interference filter variations can be effectively eliminated by the "Q-D" equation. The internal  $CO_2$  problem is minimized by selecting the proper value of E, its most sensitive variable, and finding A, B and C for optimum similarity.

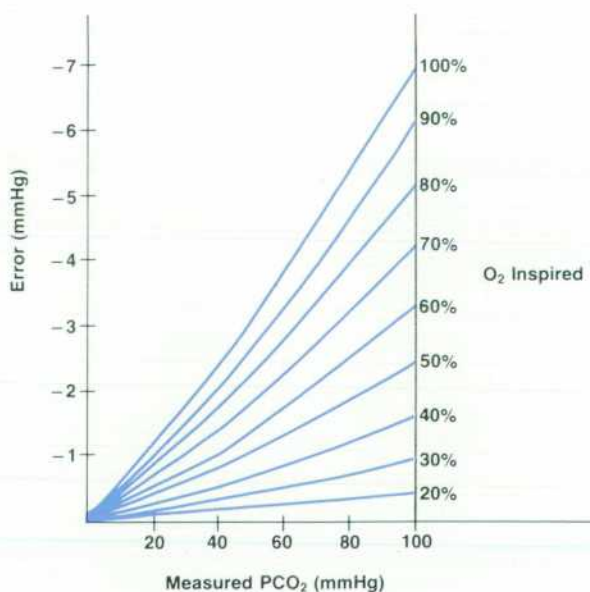


**Fig. 4.** Plots of the error in the uncompensated  $PCO_2$  value caused by interference from various oxygen concentrations.

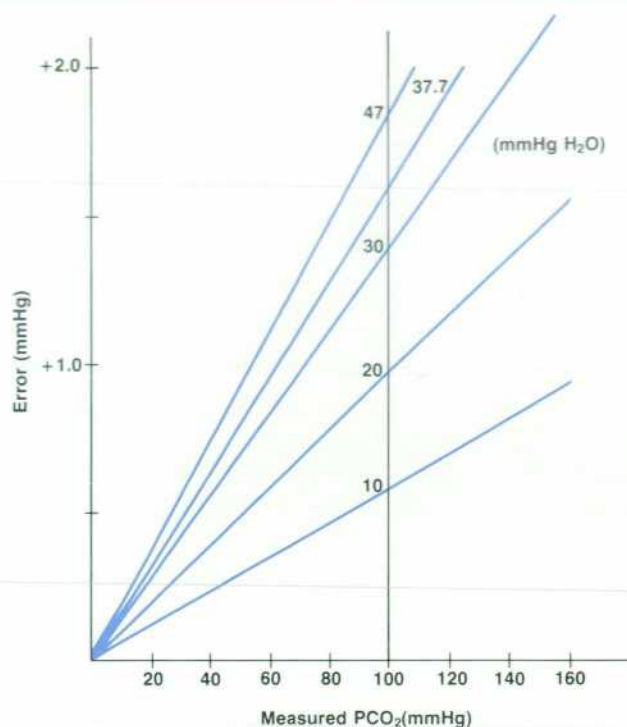


**Fig. 5.** Plots of the error in the uncompensated  $PCO_2$  value caused by the presence of various water vapor pressures.

Finding a value for E that minimizes the effect of internal  $CO_2$  is only half the solution. This internal  $CO_2$  concentration is not stable, because it varies with time and sensor temperature. To eliminate the effect of varying  $CO_2$  in the sensor, a third hole is used in the filter wheel. This third hole is an open chamber that is used as an alternate VS cell to measure the detector's output VH not only as a function of  $CO_2$  in the sample chamber but also as a function of  $CO_2$  inside the sensor. A new Q value, labeled U, is calculated from the VR:VH ratio. The normal Q, using the sealed cell, and U, using the open chamber, are compared to yield information about the concentration of  $CO_2$  inside the sensor. During calibration a  $U_0$  value and a  $U_{55}$  value as well as the  $Q_0$  and  $Q_{55}$  values are stored in an electrically alterable read-only memory (EAROM) in the 47210A.

The sensor housing  $PCO_2$  index PH is the difference between the  $PCO_2$  calculated from the Q channel and that calculated from the U channel. It is assumed, due to the integrity of the sensor sealing, that the change in internal  $CO_2$  will be slow. Therefore, while Q and U are calculated by the 47210A every 100 ms, PH is heavily filtered to provide a stable internal  $CO_2$  reading. If PH is greater than 0.5 mmHg  $CO_2$ , the  $CO_2$  values from both the Q and the U readings are used to solve a quadratic equation for the actual sample  $PCO_2$ . If PH is greater than 2 mmHg, an error code is displayed by the 47210A indicating recalibration is necessary to zero the Q and the U readings. This entire scheme compensates for changes in either direction. Namely, the system works if the sensor is calibrated with  $CO_2$  inside and drifts low afterwards or if the sensor is calibrated and then  $CO_2$  accumulates inside.

Two coefficient sets (A, B, C) are used for Q, one for  $PCO_2$  less than the calibration point and one for  $PCO_2$  greater than the calibration point. They are substantially different, and optimize the performance throughout the 0-to-100-mmHg range. Two sets of coefficients for U are also used. The remaining major variable, reference cell filling, need be controlled only within moderate tolerances during manufacture.

The final task is to characterize the sensor response to interfering gases. Gases such as water vapor, oxygen, and the anesthetic nitrous oxide, can be present in the gas sample to be measured. The sensor is calibrated by using a binary CO<sub>2</sub>-nitrogen mixture to avoid any possible chemical reactions in the calibration cells. This means that when a gas other than nitrogen is in the sample, and causes a change in the measured CO<sub>2</sub>, it will contribute to the overall system error. The task then is to characterize the sensor response so that the processor box can compensate for that added error. This error should be consistent from sensor to sensor. Verification of this was necessary. An empirical approach was taken. The special sensors discussed earlier were used on the static station. The sensor was first calibrated using binary mixtures of CO<sub>2</sub> in nitrogen. Next a mixture was introduced into the static station with the same CO<sub>2</sub> partial pressure but with some amount of interfering gas. Data was accumulated in this manner for a number of transducers with varying amounts of interfering gas and CO<sub>2</sub>.

Figs. 3, 4, and 5 are plots of this data and show the PCO<sub>2</sub> measurement errors that would occur if some form of compensation was not used. The processor box in the 47210A uses a compensation routine derived from this data to reduce these errors. The user simply specifies the presence of interfering gases by pressing the appropriate correction factor pushbuttons on the front panel of the 47210A.

#### Russell A. Parker



Russ Parker received the BS degree in chemistry from Trinity College, Hartford, Connecticut in 1967. He then attended Purdue University, West Lafayette, Indiana where he was awarded a Master's degree and a PhD degree in analytical chemistry in 1972. After working for a while as an analytical chemist and an electronics designer, Russ joined HP in 1975 and has worked on accessories for the 47210A Oximeter, the 47210A Capnometer, expanding an electroplating area, and quality control. He is co-author of

three papers about an on-line computer for chemical analysis and is a co-inventor for one pending patent on a timer/controller. Russ was born in Hartford, Connecticut and now lives in Holliston, Massachusetts. He has a 10-year-old son and enjoys photography, playing tennis and volleyball, skiing, spelunking, listening to blues music, and not jogging. His friends call him "the crazy doctor."

#### Reference:

1. "A General Multiparameter Least Squares Curve Fitting Computer Programme and some of its Applications." *Talanta*, Vol. 19, 1976, pp. 1131-1139.

of the inspired gas. These switches select any one of five possible compensation states. With no buttons engaged, the instrument assumes standard conditions and a correction for 21% inspired oxygen and saturated water vapor is implemented. This compensation is a simple factor applied to the measured value.

The compensation for O<sub>2</sub> concentrations greater than 21% and 50% is also a simple factor. The value chosen minimizes the error in each band. Thus, at one specific O<sub>2</sub> inspired concentration in each range, the added error due to interfering gases is nearly zero. A similar approach is taken for nitrous-oxide-plus-oxygen interference, the difference being that instead of a straight-line error compensation, a second-order polynomial compensation is used to fit the error characteristics of the sensor response to nitrous oxide, oxygen and water vapor more closely. These correction factors are only implemented during the operational modes of the instrument. When the calibration stick supplied with the instrument is extended, the processor box assumes a calibration check is being performed on the CO<sub>2</sub> and nitrogen-filled calibration cells. Thus no interfering gas or altitude compensation is performed.

#### Calibration

The goal of providing an instrument that is easy to use and calibrate rests partly on the software and partly on the hardware. The two-point calibration scheme requires two stable, known reference concentrations to be introduced into the sample chamber one at a time. The microprocessor must also be informed when each reference is present. The scheme uses two calibration cells similar to those used in the sensor's filter wheel, one filled with nitrogen and one filled with a CO<sub>2</sub>-in-nitrogen mixture. This CO<sub>2</sub>-in-N<sub>2</sub> mixture is used as a stable reference concentration. The calibra-

tion cells are considerably larger and have thicker windows but otherwise they are similar to the cells in the sensor's filter wheel. The thicker windows help the calibration cells survive the rigors of handling during calibration. The two cells are secured in a glass-filled polycarbonate carrier (the calibration stick) attached to the front of the processor box. In addition, there are two momentary pushbutton switches, one associated with each cell, to allow the operator to inform the processor box when the sensor is in place over that calibration cell. The system is calibrated when the sensor is changed or if the system has drifted outside the prescribed bounds. To calibrate the instrument, the calibration stick is extended (Fig. 16) and the sensor is first placed on the calibration stick over the zero cell, which contains only nitrogen. The associated button is pressed and the display shows LO CAL. After an internal delay of approximately 1½ minutes to establish thermal equilibrium, the PCO<sub>2</sub> display will read 0.0. This shows that the first calibration point has been entered into the EAROM in the instrument. Next the sensor is placed over the nitrogen-and-CO<sub>2</sub>-filled cell and its pushbutton is pressed. The display shows HI CAL for three minutes after which it shows the same value as is stamped on the calibration stick (55.2 in Fig. 16). This indicates that the second calibration point has been stored in the EAROM. The system is now calibrated and ready for use. This simple, foolproof scheme allows the operator to check the instrument accuracy or calibrate the instrument without using any other equipment such as gas bottles and their associated plumbing.

The corrected waveform can be processed to get useful respiration parameters: respiration rate, end-tidal PCO<sub>2</sub>, and inspiratory minimum PCO<sub>2</sub> (see box on page 12). These parameters can be tested against alarm limits to signal a doctor or nurse of an undesirable change in the patient's

(continued on page 20)

# Making Accurate CO<sub>2</sub> Measurements

by John J. Krieger

One of the requirements of developing any fundamental measurement, such as the partial pressure of carbon dioxide, is an absolute standard. That is, what is truth in the context of CO<sub>2</sub> exhaled by a patient? Given a sensor that can measure CO<sub>2</sub> level changes, it is necessary to calibrate its response against "truth." The problem is complicated by several variables that affect the CO<sub>2</sub> measurement.

- Total barometric pressure (or altitude). Measurement interference can come from other gases such as oxygen, water vapor, nitrous oxide, and other anesthetic gases commonly used in a medical environment.
- Charles' and Boyles' Gas Laws ( $PV=nRT$ ) govern effects caused by changes in environment, gas temperature and sample gas flow rate.
- Optical and mechanical tolerances can accumulate when interchanging system components.
- Long-term drift (aging) of system components.

One way to calibrate and verify performance of the 47210A instrument is to measure many CO<sub>2</sub> samples with all of the possible variations and combinations listed above by both a 47210A system under test and a known perfect CO<sub>2</sub> sensor. An algorithm could be developed relating the 47210A system and the perfect sensor. However, the perfect standard CO<sub>2</sub> sensor does not exist. Even a fairly good one doesn't exist. The development goal is to make the 47210A more accurate and stable than any other medical sensor. This requires the CO<sub>2</sub> standard to be at least ten times better than the 47210A accuracy and stability goals. Even analyses of gas bottles supplied by the U.S. National Bureau of

Standards (NBS) are less accurate than what is needed.

Instead, we use an indirect, but more precise technique that uses different partial pressures at constant volume and temperature. Although the NBS cannot certify gas samples accurately enough, they can certify pressure and temperature very accurately. Given a fixed volume and  $PV=nRT$ , very accurately known CO<sub>2</sub> mixtures can be made. A custom, automated static gas station was built and is used to test, calibrate, verify, and manufacture the 47210A Capnometer.

The static station (Fig. 1) consists of: (1) a stainless-steel mixing chamber, (2) an isothermal circulating-water jacket, (3) an array of solenoid-controlled valves, including a precision, electrically operated, analog mixing valve and a pneumatically operated purging valve, (4) a custom interface box to control the valves, (5) an ultra-accurate MKS Inc. manometer which is read by an HP 3455A Digital Voltmeter, (6) one or more 47210A processor boxes to function as analog-to-digital (A-to-D) converters for the one or more 14360A Sensors, and (7) an HP 9825A Desktop Computer as the static station's system controller. A series of HPL programs was written to run the static station.

The static station system was run over a period of several years to mix and record thousands of CO<sub>2</sub> sample calibration points. The results are stored on magnetic tape or disc media for analysis and algorithm development.

The construction of the static station system was an engineering project in its own right involving several engineering disciplines: mechanical, electrical, and software. The heart of the static station is the stainless-steel mixing chamber. The mixing chamber

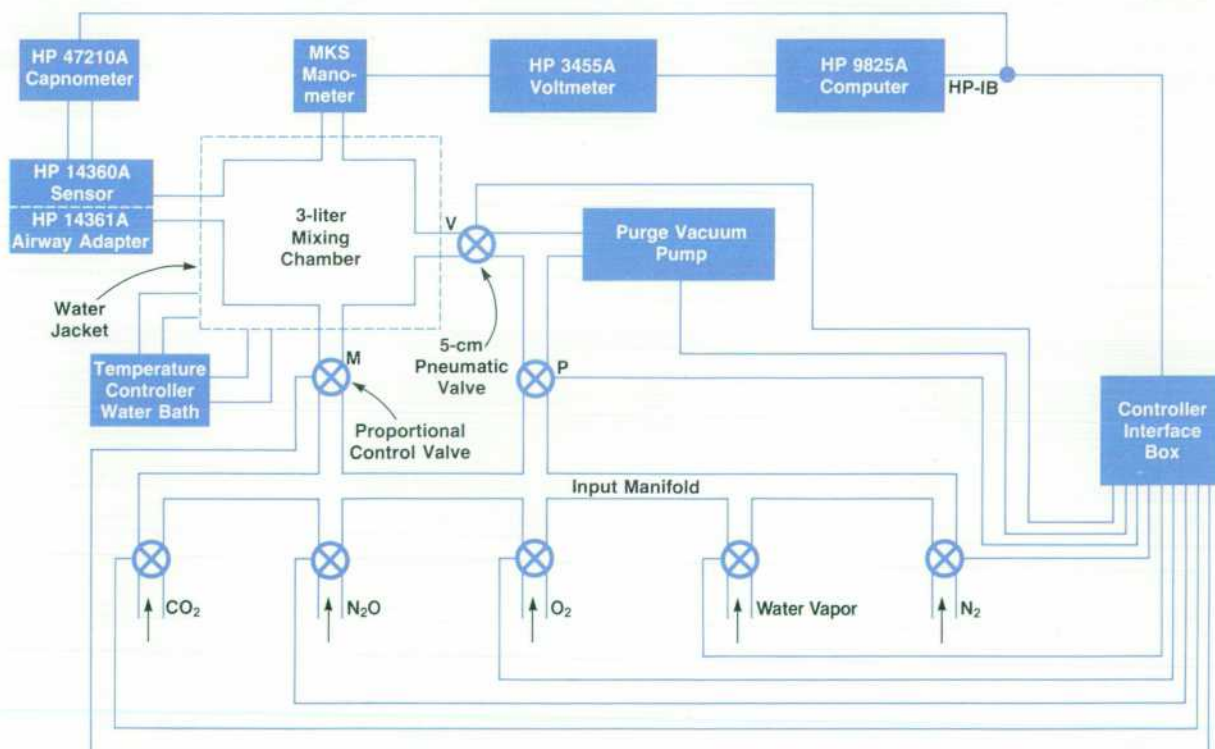


Fig. 1. Block diagram of the static station developed by HP to calibrate the 47210A Capnometer.

has several openings to external devices: the MKS Inc. manometer, the 5-cm-diameter high-vacuum purge valve, the analog mixing valve, and one or more 14361A Airway Adapter chambers. The 14360 Sensors to be calibrated are placed on the airway adapters and connected to the 47210A processor box which is used as an A-to-D converter. A special HP-IB interface board is attached to the 47210A to allow direct reading of its A-to-D converter by the 9825A Computer.

The mixing chamber is filled with various gas mixtures by the analog mixing valve M which receives one gas at a time from a manifold. The manifold is filled with either 100% carbon dioxide, nitrogen, oxygen, nitrous oxide or other commonly used operating-room anesthetic gases. The desired fraction of gas partial pressure is let into the mixing chamber. The mixing valve is then closed and the manifold is evacuated through the purging valve P. Then a different gas can be let into the evacuated manifold without fear of gas cross-contamination.

The mixing chamber is constructed of stainless steel to avoid possible chemical reactions with the gas mixtures (at one time we mixed in water vapor as one of the gases and we didn't want the mixing box to rust). Stainless steel, however, is a poor thermal conductor. For reasons that will be discussed later, the mixing chamber has to be kept at a constant temperature. This is done by completely surrounding the mixing chamber with an aluminum water jacket. A precision temperature controller and a circulating pump are coupled to the water jacket. Constant temperature is more important than accurate temperature in this application.

The airway adapters used in the static station are constructed specially to eliminate variability and assure that the accumulated data reflects nominal conditions.

A desired gas mixture sample point is orchestrated by the 9825A Computer by the proper sequencing and timing of the various valves. As an example, suppose we want to make a sample point of 55 mmHg CO<sub>2</sub>, 50% nitrous oxide, 21% oxygen, and the balance nitrogen to make a total pressure of 760 mmHg (sea level). The control sequence is as follows:

1. Vent mixing chamber for three minutes (valve V).
2. Purge manifold for one minute (valve P).
3. Let CO<sub>2</sub> into evacuated manifold.

4. Fill mixing chamber until it has a total pressure of 55 mmHg.
5. Purge manifold for one minute (valve P).
6. Let nitrous oxide into evacuated manifold.
7. Fill mixing chamber until it has a total pressure of  $55 + 50\% \times 760 = 435$  mmHg.
8. Purge manifold for one minute (valve P).
9. Let oxygen into evacuated manifold.
10. Fill mixing chamber until it has a total pressure of  $435 + 21\% \times 760 = 594.6$  mmHg.
11. Purge manifold for one minute (valve P).
12. Let nitrogen into evacuated manifold.
13. Fill mixing chamber until it has its final total pressure  $594.6 + 165.4 = 760.0$  mmHg.

The static station controller then waits until the various layers of gas form a homogeneous mixture by Brownian motion. The mixing chamber has a mixing time constant of three or four minutes, so all the nooks and crannies are equilibrated in about 10 to 15 minutes. Typically mixing and measuring each gas data point takes about 25 to 40 minutes. This computerized system makes it possible to do the routine calibration of a sensor and airway overnight and reduces the drudgery of what would otherwise have to be done manually.

The partial-pressure filling subroutine mentioned above is a complicated procedure involving feedback from the MKS Inc. manometer. The computer calculates the target pressure that the mixing chamber is to be filled with and fills it with successively smaller pressure pulses. An attempt was made to approximate an isothermal expansion. This can only be done perfectly by an infinitesimal flow rate. A quick expansion of a gas causes it to cool down (e.g., the use of Freon™ in a refrigeration system). An empirically derived algorithm was developed for the analog mixing valve that is used. At first long gas pulses at high flow rates are used. Then, as the target pressure is approached, short, low-flow-rate pulses of short duty cycle are used to creep slowly up to the target pressure. In this way, an isothermal expansion is achieved in a minimum time. The constant-temperature mixing-chamber water jacket is very important for the mixing task.



**Fig. 16.** The calibration stick supplied with the 47210A contains two cells that have reference concentrations of gas sealed in them. The sensor is placed on one cell at a time to check and calibrate the instrument.

respiration status.

The main program then displays the fully processed parameters on the capnometer's front panel and outputs the instantaneous PCO<sub>2</sub> waveform to a rear-panel analog output



#### Rodney J. Solomon

Rod Solomon joined HP in 1972 with several years of experience working with small computer peripherals, missile guidance, and photoreconnaissance. At HP he has worked on the mechanical design for an ECG monitor, led a strip-chart recorder project and served as project manager for the 47210A Capnometer. A native of Syosset, New York, Rod attended Pratt Institute in Brooklyn, New York, earning the BME degree in 1967. He is a co-inventor for a patent on an automobile anti-theft device. Rod is married, has two children, and lives in Needham, Massachusetts. He enjoys flying, tinkering with automobiles, and fixing up his 60-year-old home.

for use with chart recorders or slow-trace oscilloscopes. When the processing is completed, the data-available flag is cleared and the main program awaits the A-to-D converter's service routine to signal the arrival of the next digital data group.

### Acknowledgments

Many people at Hewlett-Packard Laboratories in Palo Alto, California laid the groundwork for the 47210A Capnometer, notably Charlie Hill and John Bridgham. At HP's Waltham Division the intricate mechanical design of the sensor assembly was performed by Ed Parnagian with assistance by Ross Frushour and John Allen. Al Bond contributed to the processor box design and the sensor manufacturing techniques. A truly superb job was done on the elec-

tronics by a trio of engineers: John Krieger, Gerry Kager and Ray Stelling. Russ Parker, our resident chemist, performed a remarkable job of characterizing the sensor. Russ' work was the key to success with the simple-to-perform calibration scheme. Tom Hayes, our gas monitoring product line manager, provided valuable guidance regarding the needs of the medical user. A final thanks goes to our section manager, Ed Merrick, who demonstrated his abilities as an exceptional engineer many times in the course of developing the 47210A. His help was greatly appreciated.

### Reference

1. B. Smallhout and Z. Kalenda, "An Atlas of Capnography," Kerckebosch, Zeist, The Netherlands, 1975.

## SPECIFICATIONS

### HP Model 47210A Capnometer

#### Measurements

##### INSTANTANEOUS PCO<sub>2</sub>:

###### ANALOG OUTPUT:

Range: 0 to 150 mmHg (0 to 7.5V).

\*Accuracy: ±2 mmHg from 0 to 40 mmHg.

±5% of reading from 40 to 100 mmHg.

Response Time: Delay, 150 ± 25 milliseconds.

Rise Time (90% rise to a PCO<sub>2</sub> step change), 200 milliseconds.

Noise: ±0.5 mmHg (rms), or 1.5% of reading, whichever is higher.

###### DIGITAL DISPLAY:

Range: 0 to 150 mmHg.

\*Accuracy: ±2.5 mmHg from 0 to 40 mmHg.

±5.5% of reading from 41 to 100 mmHg.

Response Time: Delay, 150 ± 25 milliseconds.

Rise Time (90% rise to a PCO<sub>2</sub> step change), 200 milliseconds.

##### END-TIDAL PCO<sub>2</sub>/INSPIRATORY MINIMUM PCO<sub>2</sub>

###### ANALOG OUTPUT:

RANGE: 0 to 150 mmHg (0 to 3.0V).

\*Accuracy: ±2 mmHg from 0 to 40 mmHg.

±5% of reading from 40 to 100 mmHg.

###### DIGITAL DISPLAY:

Range: 0 to 150 mmHg

\*Accuracy: ±2.5 mmHg from 0 to 40 mmHg.

±5.5% of reading from 41 to 100 mmHg.

##### RESPIRATION RATE (BPM):

###### ANALOG OUTPUT:

Range: 0 to 75 BPM (0 to 3.0V).

Accuracy: ±2 BPM (4 to 75 BPM).

###### DIGITAL DISPLAY:

Range: 0 to 75 BPM.

Accuracy: ±2 BPM (4 to 75 BPM).

##### \*Notes:

- Accuracy of End-Tidal readings applies to measurements greater than 10 mmHg.
- Standard conditions:  
Gas Mixture: CO<sub>2</sub>, N<sub>2</sub>, O<sub>2</sub> (inspired) at 21%, and water vapor.  
Temperature: 33°C (airway adapter).  
Pressure: 760 mmHg (altitude setting = 0)  
Water Vapor Pressure: 38 mmHg

##### MEASUREMENT VARIABILITY

\*\*REPEATABILITY: ±0.8 mmHg from 0 to 40 mmHg

±2% of reading from 41 to 100 mmHg

STABILITY: ±1 mmHg for 7 days at 55 ± 5 mmHg, after 30-minute warmup

\*\*Conditions: The repeatability specification applies if the same sensor, airway adapter, and capnometer are used immediately after calibration. Each gas sample measured must be at the same temperature and pressure.

**COMPENSATION:** Front-panel pushbuttons provide mean corrections for gas compositions when the inspired oxygen is other than 21%. The following tables indicate the added error at the mean gas compositions and their extremes. These added errors can be reduced to nearly zero by treating them as proportional to the difference from the mean composition. In the tables, all gas percentages are for inspired gas and standard conditions (Measurements, Note 2). In all cases, the actual PCO<sub>2</sub> is the displayed PCO<sub>2</sub> plus the error in the table. For altitude settings other than zero (sea level), add ±0.3 mmHg.

##### OXYGEN LEVEL COMPENSATION:

GAS MIXTURE: CO<sub>2</sub>/N<sub>2</sub>/O<sub>2</sub>/H<sub>2</sub>O

PCO <sub>2</sub> Level	Specified accuracies at standard conditions, with O <sub>2</sub> (inspired) at 21%. No correction is applied.	Maximum Added Error (mmHg)					
		O <sub>2</sub> > 21% Button ON		O <sub>2</sub> = 50% Button ON			
40 mmHg	±2.0 mmHg	-0.4	0	+0.4	-1.0	0	+1.0
100 mmHg	±5.0 mmHg	-1.0	0	+1.0	-2.4	0	+2.2

##### NITROUS OXIDE COMPENSATION:

ANESTHETIC GAS MIXTURE: CO<sub>2</sub>/N<sub>2</sub>O/O<sub>2</sub>/H<sub>2</sub>O

PCO <sub>2</sub> Level	Specified accuracies at standard conditions, but O <sub>2</sub> (inspired) is 35%, and balance is N <sub>2</sub> O. No correction is applied.	Maximum Added Error (mmHg)					
		O <sub>2</sub> > 21% Button ON N <sub>2</sub> O Button ON		O <sub>2</sub> = 50% Button ON N <sub>2</sub> O Button ON			
40 mmHg	±2.0 mmHg	N/A	0	-0.7	+0.6	0	-0.6
100 mmHg	±6.0 mmHg	N/A	0	-1.8	+1.5	0	-1.5

#### General

##### REAR PANEL 780 SYSTEM CONNECTOR OUTPUT:

Connector pin assignments are compatible with standard signal lines in the Hewlett-Packard Patient Monitoring Series.

##### OPERATING ENVIRONMENT:

###### AMBIENT TEMPERATURE RANGE:

Capnometer: 0°C to 55°C

14360A Sensor: 17°C to 38°C

###### HUMIDITY:

Capnometer: 5% to 95% relative humidity at 40°C

14360A Sensor: 5% to 95% relative humidity at 38°C

##### ELECTRICAL:

LINE VOLTAGE: 100, 120, 220, 240Vac.

+5% - 10%, 50 to 60 Hz.

POWER CONSUMPTION: 50 VA maximum.

CHASSIS LEAKAGE CURRENT TO GROUND: Less than 50 microamperes at 127Vac, 60 Hz.

PATIENT ISOLATION FROM INSTRUMENT GROUND: Greater than 10 megohms measured from 14360A sensor case to power-cord third-wire ground at 40°C and 95% relative humidity.

INPUT PROTECTION: Protected against defibrillator potentials. Free from electrocautery interference under most circumstances.

##### MECHANICAL:

DIMENSIONS: Capnometer (HWD): 19.1 × 21.3 × 38.1 cm.

SENSOR CABLE LENGTH: 2.44 m.

AIRWAY ADAPTER LENGTH (with tubing couplers): 9.5 cm.

TUBING COUPLERS (ANSI Standard Z79): 15-mm diameter.

WEIGHTS: Capnometer: 7.7 kg.

SENSOR: 56 g without cable

195 g with cable

AIRWAY ADAPTER: 18 g with tubing couplers.

STERILIZATION: Capnometer may be wiped with cold chemical disinfectant. Sensor may be sterilized with buffered glutaraldehyde. Airway adapter less disposable tubing couplers may be autoclaved, gas sterilized (ethylene oxide), or cold-chemical sterilized.

DEAD SPACE: Airway Adapter (with tubing couplers): 15cc.

PRICE IN U.S.A.: \$6,400.

MANUFACTURING DIVISION: WALTHAM DIVISION

175 Wyman Street

Waltham, Massachusetts 02154 U.S.A.

# A Versatile Low-Frequency Impedance Analyzer with an Integral Tracking Gain-Phase Meter

*This instrument measures impedance parameters, gain, phase, and group delay of individual components, circuit sections, and complete circuits. The measurements are automatic, wideband, and made under variable frequency and/or dc bias voltage conditions.*

by Yoh Narimatsu, Kazuyuki Yagi, and Takeo Shimizu

**T**HE DEVELOPMENT of more complex electronic systems and components requires improved instrumentation to evaluate impedance and transmission characteristics of individual components and circuits. Ideally, this evaluation should be done under the conditions of frequency, bias, and signal level at which the device or circuit is to operate.

Measuring both impedance and transmission parameters usually requires at least two instruments: an analog vector impedance meter or a digital LCR meter to measure impedance parameters, and a gain-phase meter or network analyzer to measure transmission characteristics.

Hewlett-Packard's Model 4192A LF Impedance Analyzer (Fig. 1) introduces a new concept in the measurement of these parameters. To our knowledge, it is the industry's first fully automatic, wideband, variable-frequency, multi-parameter impedance meter that is equipped with a tracking gain-phase meter. It can also measure group delay and

be operated via the HP-IB.\* The 4192A is designed to simplify and improve the testing of discrete complex devices and in-circuit components, and the evaluation of circuits, materials, and semiconductor products. Some of its features are:

- All measurements and test conditions are specified with pushbutton ease. There are no knobs or dials to adjust. An internal microprocessor can automatically select the measurement range and circuit mode (equivalent series or parallel) appropriate for the specified conditions and measured parameter value.
- Eleven impedance parameters ( $|Z|$ ,  $|Y|$ ,  $\theta$ , R, X, G, B, L, C, D, and Q) can be measured. Equivalent series or parallel mode is selectable manually or automatically.
- Test signal frequency can be automatically or manually swept in either direction within a range of 5 Hz to 13 MHz. A fixed test signal frequency can be specified any-

\*Hewlett-Packard's implementation of IEEE Standard 488 (1978).



**Fig. 1.** The 4192A LF Impedance Analyzer makes accurate measurements of impedance and gain-phase response for components, materials, and two-port devices in the frequency range of 5 Hz to 13 MHz. Test signal levels are programmable. The analyzer has frequency-sweep capability, 4½-digit resolution, built-in dc bias that can be swept, and X-Y recorder outputs.

where within that range with a resolution better than 0.0001%.

- Test signal amplitude is selectable from 0.005 to 1.100 Vrms in steps as small as 1 mV. The actual test signal amplitude across the device under test (DUT) can be monitored by the 4192A.
- An internal  $\pm 35$ Vdc bias source can be automatically or manually swept in 10-mV steps.
- Five gain-phase parameters ( $|B-A|$ ,  $\theta$ , group delay,  $|A|$ , and  $|B|$ ) can be measured with a maximum gain resolution of 0.001 dB and a phase resolution of  $0.01^\circ$ . The dynamic range for the input level is 100 dB and the level can be measured in dBm or dBV.
- X-Y recorder outputs between zero and  $\pm 1$ V. These outputs are driven by digital-to-analog converters (DACs) controlled by the instrument's microprocessor. The consistent output ramp simplifies recorder setup.
- An internal backup memory, consisting of five non-volatile storage registers, stores all of the settings for up to five independent measurement setups.

All front-panel keys and test parameter settings can be controlled by means of the instrument's HP-IB capability.

The 4192A LF Impedance Analyzer is part of HP's variable-frequency impedance analyzer family. It covers the frequency range below that of the 4191A RF Impedance Analyzer<sup>1</sup> which does impedance measurements in the HF to UHF frequency range. Together the 4191A and 4192A can make impedance measurements over the very wide frequency range of 5 Hz to 1 GHz.

The main applications for the 4192A are testing of complex discrete components, either separately or in-circuit, and evaluating circuits, materials, and semiconductor devices. An example is measuring quartz crystal parameters. Manufacturers and users of quartz crystals require an accurate way to measure a crystal's series or parallel resonant frequency, equivalent series resistance, shunt capacitance, and Q. The 4192A can perform all these measurements quickly. If an HP-IB controller is available, they can be made

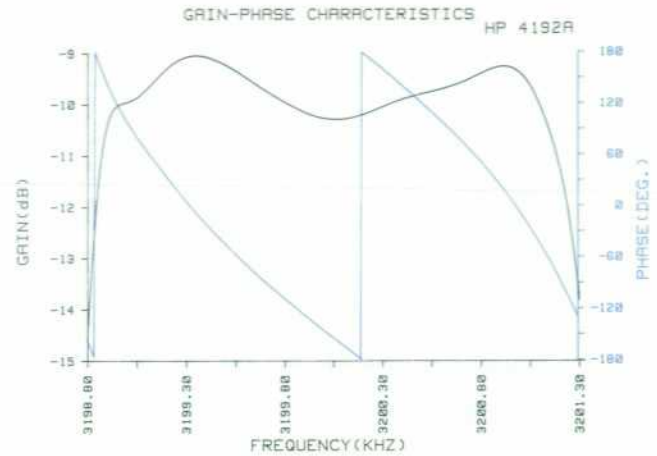


Fig. 3. Gain-phase characteristics of a 3.2-MHz crystal filter in its passband are measured easily by the 4192A.

automatically and plotted graphically (Fig 2). If an X-Y recorder is connected to the 4192A's recorder outputs, measurement results can be recorded on standard logarithmic or linear graph paper.

When used with an HP-IB controller, the 4192A can automatically measure the frequency characteristics of cored inductors while keeping the test current through the DUT constant. This is possible because the output level of the signal source can be remotely controlled while monitoring the test signal level.

Unlike most impedance measurement instruments, the 4192A can measure the input or output impedance of devices and circuits grounded on one side, such as filters and amplifiers.

The combination of impedance and gain-phase measurement capabilities provides many benefits, especially in designing video, communication, and hybrid IC circuits. The greatest benefit is that the designer can evaluate both

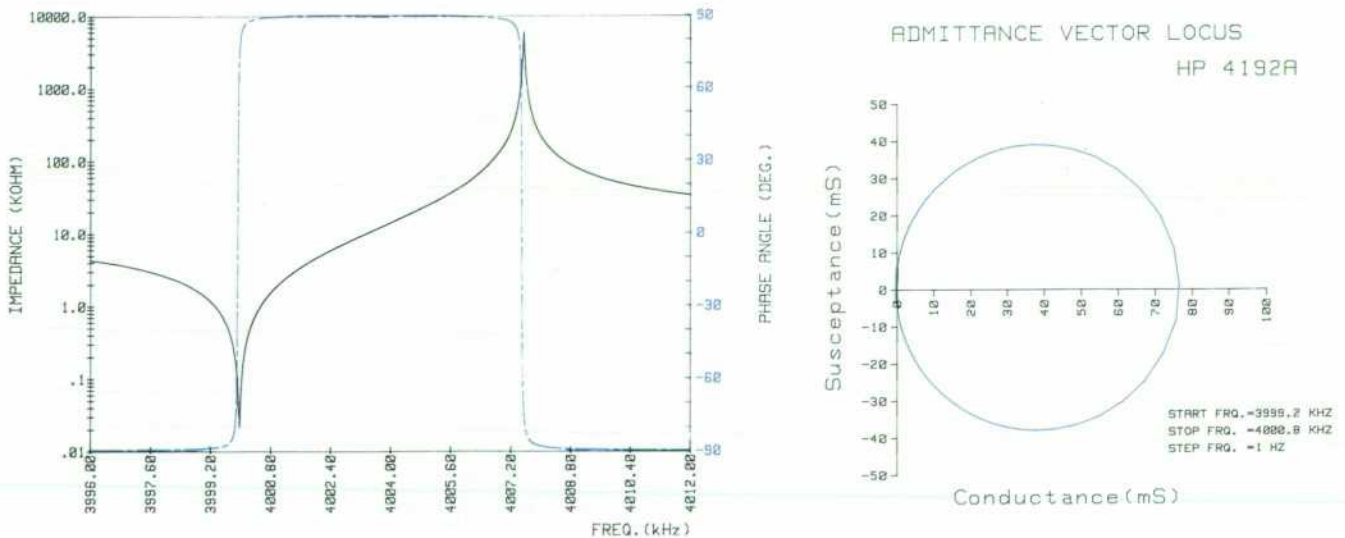


Fig. 2. (a) Impedance characteristics of a 4-MHz quartz crystal, measured with the 4192A LF Impedance Analyzer. (b) Admittance vector locus of the 4-MHz quartz crystal near the series-resonance frequency.

the characteristics of an entire circuit and the impedance characteristics of the components that make up the circuit. For example, Fig. 3 shows measurements made on a crystal filter, and Fig. 2 shows measurements on a crystal. Therefore, the designer can precisely analyze circuit performance down to the component level. The 4192A also makes it possible to troubleshoot and upgrade the circuit easily. This not only improves design efficiency, but also contributes to reliable design.

### LF Bridge

The major sections of the low-frequency impedance analyzer are the LF bridge, the vector ratio detector, the signal source, and the digital data and control section.

The bridge section (Fig. 4) in the 4192A uses an approach different from that used in similar instruments like HP's 4274A and 4275A Multifrequency LCR Meters.<sup>2</sup> For impedance measurements this section provides a complex voltage across the device under test (DUT) and another complex voltage proportional to the complex current through the DUT at bridge balance.

A heterodyne method is used to balance the bridge over the frequency range of 5 Hz to 13 MHz. The bridge uses two mixers. One is placed right after the I-V converter and the other at the front of the low current amplifier. Therefore, the IF amplifier and the null detector can operate at the intermediate frequency (78.125 kHz) regardless of the measurement frequency and the vector generator can operate at 40 MHz. Thus, it is easy to obtain two 90° phase shifters to drive the null detector and the vector generator. This made

it possible to design a simplified digital phase tracking circuit.

The I-V converter, filter, low current amplifier, and measurement cables cause a phase shift large enough to prevent the bridge from balancing at high measurement frequencies. This phase shift has to be compensated appropriately so that the bridge can be balanced over the full frequency range. A phase shift between the reference signal of the null detector and the IF signal causes a phase shift between the bridge input ( $L_{POT}$ ) and output ( $L_{CUR}$ ) in Fig. 4, provided that the phases of the local, 40-MHz, and VCO signals are kept constant. A digital phase tracking circuit varies the phase shift of the reference of the null detector. It consists of a preset binary counter and latches. If one pulse of the 16IF signal is removed from the input pulses during each period of the IF signal, the reference phase of the null detector can be delayed 22.5° from the IF signal. The phase tracking data is programmed according to the measurement frequency and cable length, and is stored in a ROM for use by the instrument's microprocessor.

The bridge of the 4192A uses a four-terminal-pair configuration<sup>3</sup> to avoid measurement errors caused by mutual inductance between measurement cables. Errors can be avoided because the magnetic fields generated by the currents flowing in the inner and outer conductors of the measurement cable cancel each other when the bridge is balanced. To maintain this condition over the full test frequency range, the bridge section uses floating power supplies for the low current amplifier, the I-V converter, and the coaxial baluns. The floating power supplies pro-

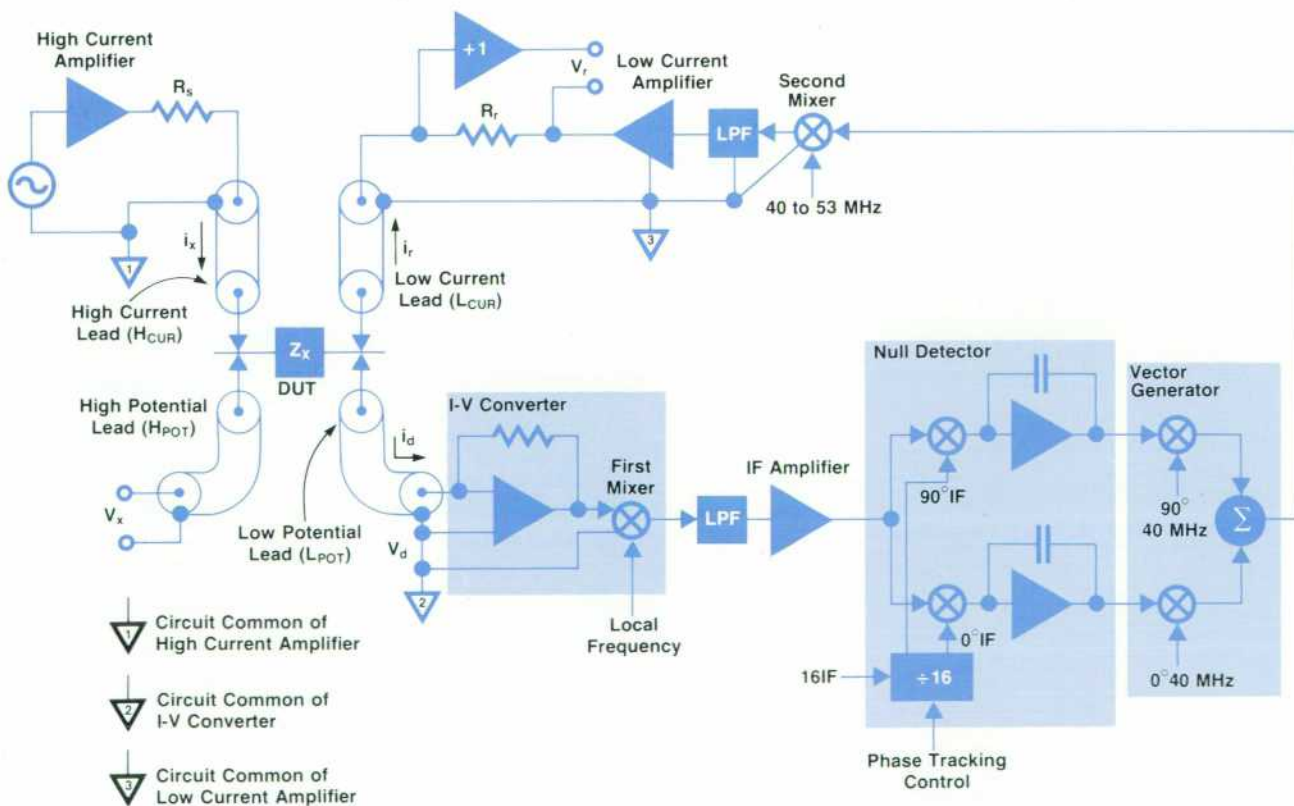


Fig. 4. Bridge section of the 4192A. The high current, low current and I-V converter sections each have an independent floating power supply to make measurement of one-side-grounded devices possible.

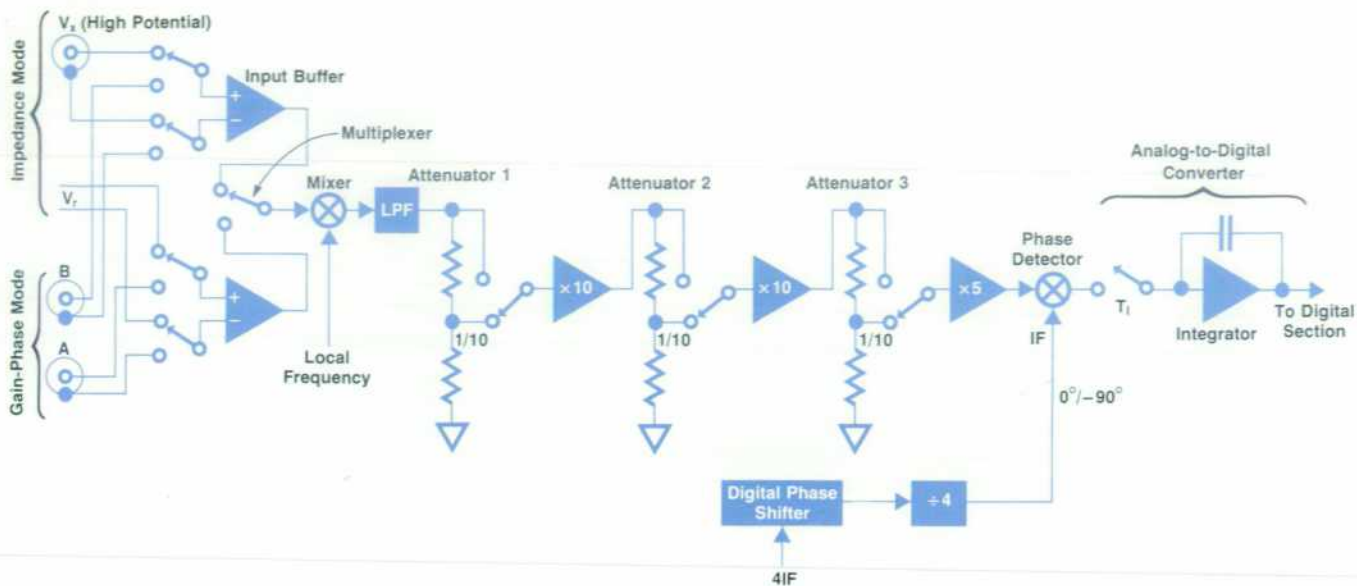


Fig. 5. Vector ratio detector. This circuit uses only one frequency conversion.

vide excellent isolation between the low current amplifier and the I-V converter and chassis ground. Each power supply is a dc-to-dc converter with a 1-MHz switching frequency and low-pass filters. Common-mode noise is approximately 10  $\mu$ V rms. These floating supplies provide the grounded-on-one-side impedance measurement capability.

If the bridge is unbalanced, an error current  $i_d$  flows into the I-V converter and is converted into an IF error signal by the first mixer. The amplified IF error signal is added to the null detector to control the 40-MHz vector generator. The signal converted from the 40-MHz error signal is fed back to the other side of the reference resistor until the system becomes balanced, that is, until  $i_d = 0$  and  $V_d = 0$ .

$$\frac{V_x}{Z_x} = i_x = i_r = -\frac{V_r}{R_r}$$

$$\text{Therefore } Z_x = -R_r \frac{V_x}{V_r}$$

As seen from the above equation, all that is needed to calculate the complex impedance of the DUT are the values of  $R_r$  and the vector ratio between  $V_x$  and  $V_r$ .

### Vector Ratio Detector

Fig. 5 shows a simplified block diagram of the vector ratio detector section. This section detects the precise complex voltage ratio (both magnitude and phase difference ratios) between two signals.

To obtain good tracking characteristics and linearity for various test signal levels, the buffered signals are multiplexed in a timesharing manner to share one signal path. The output from the multiplexer is converted into an IF signal by a mixer to cover the measurement frequency range from 5 Hz to 13 MHz. Typical tracking accuracy is 0.03% for midrange frequencies and 0.3% for the high and low frequencies. The equivalent input noise of the mixer is low

enough to allow detection of weak signals, especially for gain-phase measurements. Maximum input level is approximately 2V rms.

To satisfy these requirements, field-effect transistor switches and operational amplifiers are used to provide a double-balanced mixer having a wide dynamic range (Fig. 6). Compared with conventional diode mixers, this mixer exhibits much better linearity for high input levels and lower power requirements for the local port. The equivalent input noise is about the same as that of the operational amplifiers. To keep the signal level for the analog-to-digital converter (ADC) constant in the impedance measurement mode, the signal conversion gain of the mixer is controlled according to the test signal level.

Besides the desired feedthrough component, several un-

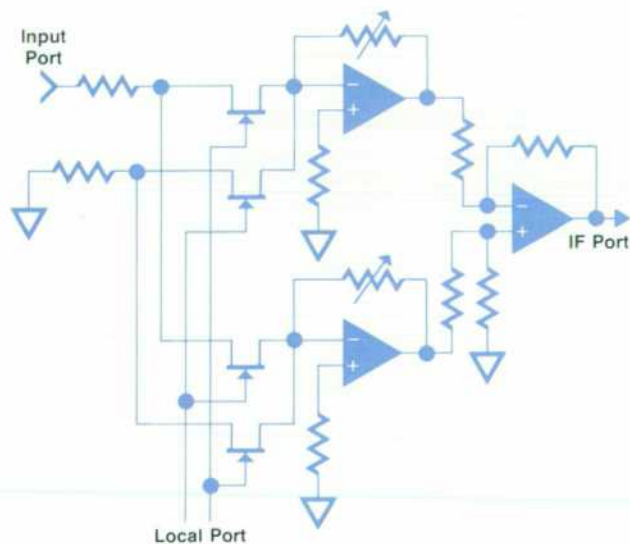


Fig. 6. Double-balanced mixer provides good linearity over the entire operating range.

wanted signals are also applied to the IF stage from the IF port of the mixer. Examples are the sum of the signal and the local signal, feedthrough from the local port to the IF port of the mixer, and sideband noise introduced around the IF signal by various noise sources. Conventional methods to eliminate these unwanted components use a high-Q bandpass filter in the IF stage. If this approach is used, the frequency components as near as 10 Hz from the IF must be attenuated by more than 80 dB. Such high-Q filters are very costly and introduce a significantly slower response to input level changes. Therefore, a different approach was chosen in the 4192A for filtering.

The integration time of the ADC is used as a filter function. It is well known that an integrator whose integration time is  $T_I$  has a frequency response  $F_f$  as follows:

$$F_f = \frac{\sin(\pi f T_I)}{\pi f T_I}$$

where  $f$  is the input frequency.

Since the phase detector located in front of the integrator is regarded as a mixer whose input component is mixed with the IF signal, the unwanted components described above (except sideband noise) are converted to components whose frequencies are multiples of the measurement frequency. Therefore, if  $T_I$  is set to be a multiple of the reciprocal of the measurement frequency, the term  $\sin(\pi f T_I)$  becomes zero and unwanted components are eliminated. The higher the measurement frequency becomes, the further the unwanted components appear from the IF signal. The IF filter (following the mixer in Fig. 5) becomes effective only for measurement frequencies above 10 kHz. Consequently, rejection by using an integration time  $T_I$  is especially necessary for the lower measurement frequencies.

$T_I$  is varied by changing the integration time counter via the microprocessor. Since the integration time must vary from approximately 2.5 ms to 600 ms, an ordinary dual-slope integrator cannot be used because of its limited dynamic range. An integrator similar to the one used in the

HP 3455A Digital Voltmeter<sup>4</sup> is used, because its dynamic range is practically infinite.

The noise bandwidth of filters of this type is equal to the reciprocal of the integration time. For example, an integration time of 20 ms gives a noise bandwidth of 50 Hz. This is approximately equal to the noise bandwidth of a filter with a -3-dB bandwidth of 32 Hz if the filter is approximated by a single-tuned bandpass filter having a Q of 2400.

### Signal Source

Fig. 7 shows a simplified block diagram of the 4192A's signal source section. In impedance measurements or gain-phase measurements, a good quality test signal is essential for obtaining high-resolution measurements with good repeatability. The basic concept used in the 4192A is to phase-lock the 40-to-53-MHz signal from VCO #1 to a 100-kHz signal that is divided down from a 40-MHz signal by using fractional-N frequency synthesis.<sup>5</sup> The VCO #1 output is then converted to the 5-Hz-to-13-MHz test signal by mixing.

A local frequency that is always higher than the test signal frequency by the IF (usually 78.125 kHz) is obtained by subtracting the 40-MHz-IF signal from the VCO #1 output. The 40-MHz-IF signal is generated by VCO #2 which is phase-locked to the IF frequency divided from the 40-MHz signal. Leveling of the output signal is achieved by feeding back an ALC (automatic level control) signal to the PIN modulator inserted in the path of the 40-MHz signal. Control of output level is achieved by changing the reference level of the ALC loop, which is controlled by an 8-bit digital-to-analog converter (DAC).

### Digital Circuitry

All data and analog controls are managed by an MC68B00 microprocessor. A battery-supported backup memory retains five independent instrument setups when the instrument is turned off or line power is removed. Troubleshooting is done easily with the instrument's built-in test capability and a specially designed troubleshooting kit that is

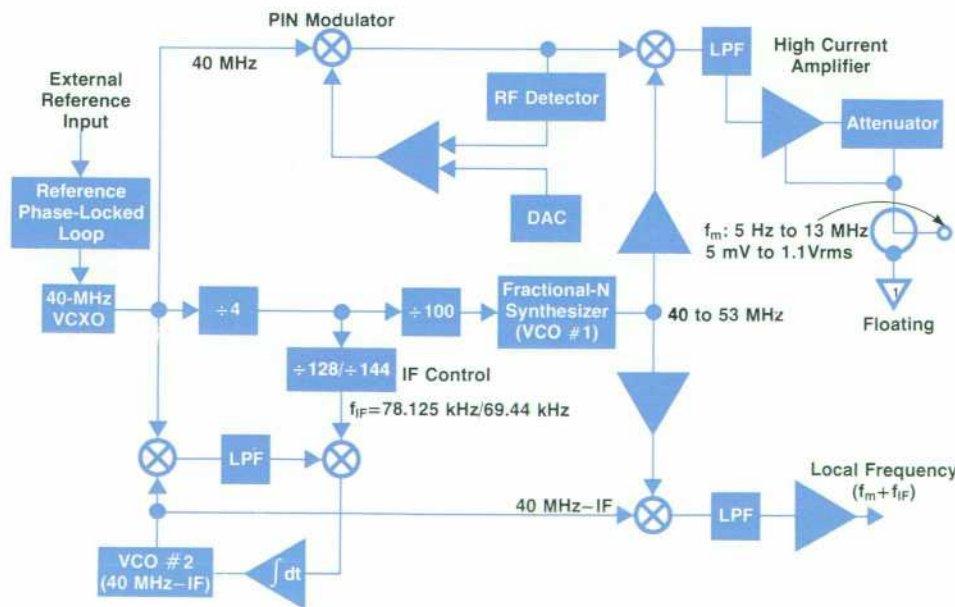
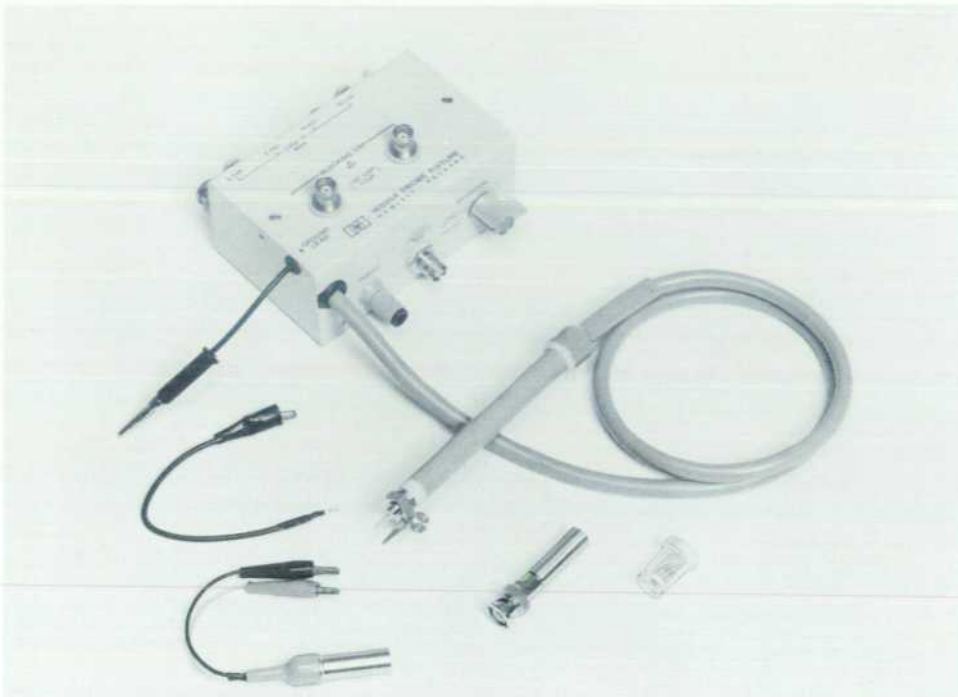
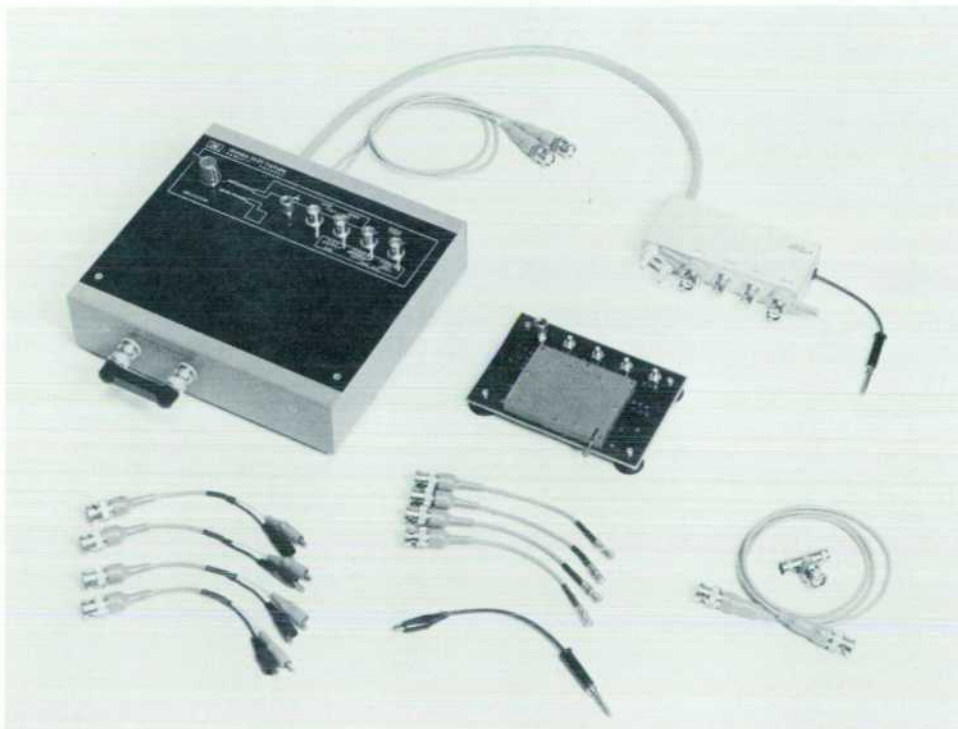


Fig. 7. The signal source section of the 4192A generates the test and local signals by using a fractional-N synthesizer.



**Fig. 8.** The 16095A probe fixture is useful for probing circuits and devices grounded on one side.



**Fig. 9.** The 16096A test fixture is useful for measurements of two-port devices and circuits.

supplemented by signature analysis.

### Test Fixtures

Two different types of test fixtures and an accessory kit are available for circuit probing or measurement of two-port devices. Also, most of the test fixtures usable with HP's 4274A and 4275A Multifrequency LCR Meters can be used with the 4192A.

The 16095A probe test fixture (Fig. 8) is convenient for measurement of devices grounded on one side, circuits, and in-circuit components. Before using the probe, zero offset compensation should be performed to cancel the effects of any residual inductance and stray capacitance inherent in the probe fixture.

The 16096A test fixture (Fig. 9) is used to measure the input/output impedance and gain-phase response of two-port devices and circuits.

## SPECIFICATIONS

### HP Model 4192A LF Impedance Analyzer

#### PARAMETERS MEASURED:

IMPEDANCE PARAMETERS:  $|Z|$ ,  $-\theta$ ,  $|Y|$ ,  $-\theta$ , R-X, G-B, L-R, G, D, Q, C-R, G, D, Q relative gain (B-A), phase, group delay, absolute gain (A, B).

GAIN-PHASE PARAMETERS: (B-A)- $\theta$ , (B-A)-group delay, A, B.

**DEVIATION MEASUREMENT:** Displays measured value as deviation ( $\Delta$ ) from stored reference or as percent deviation ( $\Delta\%$ ) for all parameters.

**TEST SIGNAL** (Internal synthesizer):

FREQUENCY RANGE: 5.000 Hz to 13.000000 MHz.

FREQUENCY STEPS: 1 mHz (5 Hz to 10 kHz), 10 mHz (10 to 100 kHz), 100 mHz (100 kHz to 1 MHz), 1 Hz (1 to 13 MHz).

FREQUENCY ACCURACY:  $\pm 50$  ppm.

SIGNAL LEVEL (open-circuit for impedance measurement or terminated with 50 $\Omega$  for gain-phase measurement): 5 mV to 1.1Vrms.

**MEASUREMENT MODE:**

SPOT MEASUREMENT: Measurements at specific frequency or bias voltage.

SWEEP MEASUREMENT: Linear or logarithmic sweep measurements.

**INPUT IMPEDANCE OF CHANNEL A AND B:** 1 M $\Omega$   $\pm 2\%$  in parallel with 25 pF  $\pm 5$  pF.

**MEASUREMENT RANGE AND BASIC ACCURACY:**

Parameter	Range*	Basic Accuracy**
Impedance $ Z $	0.1 m $\Omega$ to 1.2999 M $\Omega$	0.2%
Admittance $ Y $	1 nS to 12.99 S	0.2%
Phase	-180.00° to +180.00°	0.1°
Relative Gain (B-A)	0.001 dB to 100 dB	0.02 dB
Group Delay	0.1 ns to 10 s	Calculated by accuracy of phase
Absolute Gain A, B	13.8 dBm to -87 dBm (50 $\Omega$ ) 0.8 dBV to -100 dBV	0.4 dBm 0.4 dBV

\*Varies depending on measurement frequency and test signal level.

\*\*Basic mainframe accuracy. At frequencies below 400 Hz and above 1 MHz, the basic mainframe accuracy begins to roll off.

**CIRCUIT MODE:** Series, parallel, and automatic.

**MEASURING TERMINALS:** 4-terminal pair configuration.

**DISPLAYS:** 4½-digit display in average and normal mode. 3½-digit display in high-speed mode.

**INTERNAL DC BIAS:** -35V to +35V, 10-mV steps.

**RECORDER OUTPUTS:** -1V to +1V for display A and B. 0 to 1V for frequency/bias, 1-mV steps.

**MEASURING TIME:**

IMPEDANCE MEASUREMENT: 140 to 170 ms (60 to 90 ms in high-speed mode).

GAIN-PHASE MEASUREMENT: 180 to 220 ms (90 to 130 ms in high-speed mode).

**GENERAL:**

OPERATING TEMPERATURE: 0 to 55°C, 95% relative humidity at 40°C.

POWER: 100, 120, 220V  $\pm 10\%$ , 240V  $+5\%$ ,  $-10\%$ , 48 to 66 Hz.

POWER CONSUMPTION: 100VA maximum.

DIMENSIONS APPROXIMATE (HWD): 247 mm  $\times$  425 mm  $\times$  547 mm.

WEIGHT: Approximately 19 kg.

ACCESSORIES FURNISHED: 16047A Test Fixture, two 11048C 50 $\Omega$  feedthroughs, 11652-60009 50 $\Omega$  Power Splitter, 1250-0216 BNC Adapter, and two 11170A Cable Assemblies.

ACCESSORIES AVAILABLE: 16095A Probe Fixture, 16096A Test Fixture, 16097A Accessory Kit, 16047B/C Test Fixtures, 16048A/B/C Test Leads and 16034B Test Fixture.

**PRICE IN U.S.A.:** \$11,550.

**MANUFACTURING DIVISION:** YOKOGAWA HEWLETT-PACKARD LTD.

9-1, Takakura-cho  
Hachioji-shi, Tokyo, Japan

### Acknowledgments

The 4192A design team members who deserve special recognition are Seiichi Kikuta and Tomio Wakasugi, signal source section, Kiyoshi Suzuki, power supply, Masahiro Yokokawa and Eiichi Nakamura, digital section and the software, Tetsuya Shiraishi, mechanical design, Hiroshi Shiratori, test fixtures, and Tsuneji Nakayasu, industrial design.

Special thanks are also due Masahide Nishida for his general management and encouragement, and to Shiro Kito who gave much useful advice and encouragement to the team.

### References

1. T. Ichino, H. Ohkawara and N. Sugihara, "Vector Impedance Analysis to 1000 MHz," Hewlett-Packard Journal, January 1980.
2. K. Maeda and Y. Narimatsu, "Multi-Frequency LCR Meters Test Components Under Realistic Conditions," Hewlett-Packard Journal, February 1979.
3. K. Maeda, "An Automatic Precision 1-MHz Digital LCR Meter," Hewlett-Packard Journal, March 1974.
4. A. Gookin, "A Fast-Reading, High-Resolution Voltmeter that Calibrates Itself Automatically," Hewlett-Packard Journal, February 1977.
5. D. Danielson and S. Froseth, "A Synthesized Signal Source with Function Generator Capabilities," Hewlett-Packard Journal, January 1979.

#### Yoh Narimatsu



Yoh Narimatsu joined Yokogawa-Hewlett-Packard in 1971. After several years as a development engineer, he transferred to HP's Santa Clara Division and was involved in the development of the 5342A Counter. He worked on the 4275A LCR Meter and designed the vector ratio detector section of the 4192A Impedance Analyzer. Yoh holds a BSEE degree from Kyoto University and an MSEE from Stanford University. He enjoys playing volleyball and tennis, is married, and has a two-year-old son.

#### Kazuyuki Yagi



Kazuyuki Yagi joined Yokogawa-Hewlett-Packard in 1973 just after receiving his BSEE from Tokyo Institute of Technology. After a few years as a development engineer, he transferred to HP's Stanford Park Division in 1976 and was involved in the development of the 8656A Synthesized Signal Generator. During his stay in California, he received his MSEE from Stanford University. He designed the bridge section of the 4192A Impedance Analyzer. He is married and has a two-year-old daughter and a one-year-old son. He enjoys playing Shogi, Igo, and ping-pong in his spare time.

#### Takeo Shimizu



Takeo Shimizu received his BSEE from Fukui University, Japan in 1961 and joined Yokogawa Electric Works as an R&D engineer. He joined Yokogawa-Hewlett-Packard in 1964. He worked on the 4270A Automatic Capacitance Bridge and served as a project leader for several other projects before becoming project leader of the 4192A. He is married, has two sons, and enjoys playing golf.

# A Fast, Programmable Pulse Generator Output Stage

*A new pulse generator supplies fast-transition pulses for testing 100k ECL, advanced Schottky TTL, and other fast logic families.*

by Peter Aue

**W**ITH THE INTRODUCTION of fast new integrated circuit logic families like 100k ECL (emitter-coupled-logic) and the ongoing development of current technologies such as Schottky TTL and advanced Schottky TTL, the volume of fast integrated circuits is increasing rapidly. Characterization of the parameters of such ICs in R&D, production, incoming inspection, or production testing of modules designed with these circuits requires a fast, accurate pulse generator with variable transition times to match those of the logic family under test. A new HP-IB programmable pulse generator, Model 8161A (Fig. 1), allows these measurements to be performed under remote control. Increased throughput, decreased development time, and easier long-term reliability tests are among the benefits of this 100-MHz pulse generator with 1.3-ns transition times (Fig. 2).

## Design Approach

Because major portions of the proven 8160A Programma-

ble Pulse Generator<sup>1</sup> were perfectly suitable for the new instrument, the basic mechanical design, power supply and timing circuitry of the 8160A were adopted. Only minor changes were necessary to meet the needs of the 8161A's 100-MHz repetition rate and the different internal supply currents. The microprocessor hardware was redesigned to implement signature analysis and the latest-design ROMs. The major challenge was the design of the programmable transition time generator and output amplifier.

## Transition Time Generator

The main parts of the transition time generator are the current-switching differential amplifier, the clamp voltage circuitry, two buffer amplifiers, and seven high-precision current sources (see Fig. 3). To achieve the fast transition times, push-pull differential circuitry was chosen.

To describe the basic principles of operation, let's assume the four switching current sources are off and Q1 has been off and Q2 on for a long period of time. In this case  $I_{sum} =$



**Fig. 1.** Model 8161A Programmable Pulse Generator produces pulses with amplitudes up to 5V and transition times of 1.3 ns to 900  $\mu$ s, at rates up to 100 MHz. Programming is done manually using the front-panel keyboard or remotely via the HP-IB (IEEE 488).

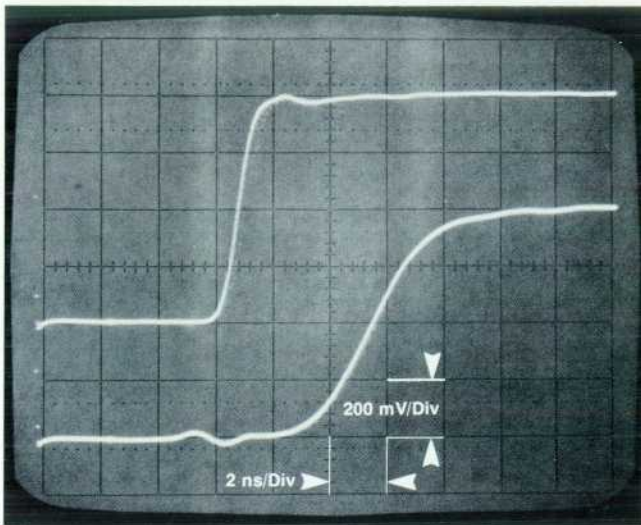


**Fig. 2.** Model 8161A's 1.3-ns transitions (upper trace) are faster and cleaner than most fast logic families, such as 10k ECL (lower trace).

$I_{LEE} + I_{TRE}$  flows through Q2. Voltage  $V_{C1} = V_1 \approx V_{CL1} + 0.7V$  and voltage  $V_{C2} = V_2 \approx V_{CL2} - 0.7V$ . When Q1 is switched on and Q2 off,  $I_{sum}$  flows through Q1 and C1 is discharged with  $I_{LEE} - I_{sum} = -I_{TRE}$ . On the other hand, C2 is charged

with  $I_{TRE}$ , since Q2 is off. When Q1 is switched off and Q2 on again, C1 is charged with  $I_{LEE}$  and C2 is discharged with  $I_{TRE} - I_{sum} = -I_{LEE}$ . The voltage swing between  $V_1$  and  $V_2$  is limited by  $V_{CL1} - V_{CL2} + 1.4V$ , which is approximately 2V. The slew rate is proportional to  $I_{LEE}$  or  $I_{TRE}$ . Therefore, with increasing current values, the transition times decrease.

C1 and C2 consist of intrinsic and stray capacitances only. The ramp signal is buffered and amplified using buffer amplifier 1. For transitions between 5 ns and 99.9 ns fixed capacitances are switched in by turning the four switched current sources on. In this case part of the signal goes through buffer amplifier 2. For transitions longer than 99.9 ns, additional capacitances are switched in.

The  $I_{LEE}$  and  $I_{TRE}$  current sources are controlled by two 10-bit multiplying digital-to-analog converters (DACs) for transitions  $\geq 5$  ns. For shorter transition times, a separate custom-designed DAC is used because the control doesn't follow a simple function and has to be approximated.  $I_{LEE}$  and  $I_{TRE}$  are made equal to achieve a cleaner waveform.

### Output Stage

A dual cascode differential amplifier (Fig. 4) drives the complementary outputs. (In the Option 020 dual-channel

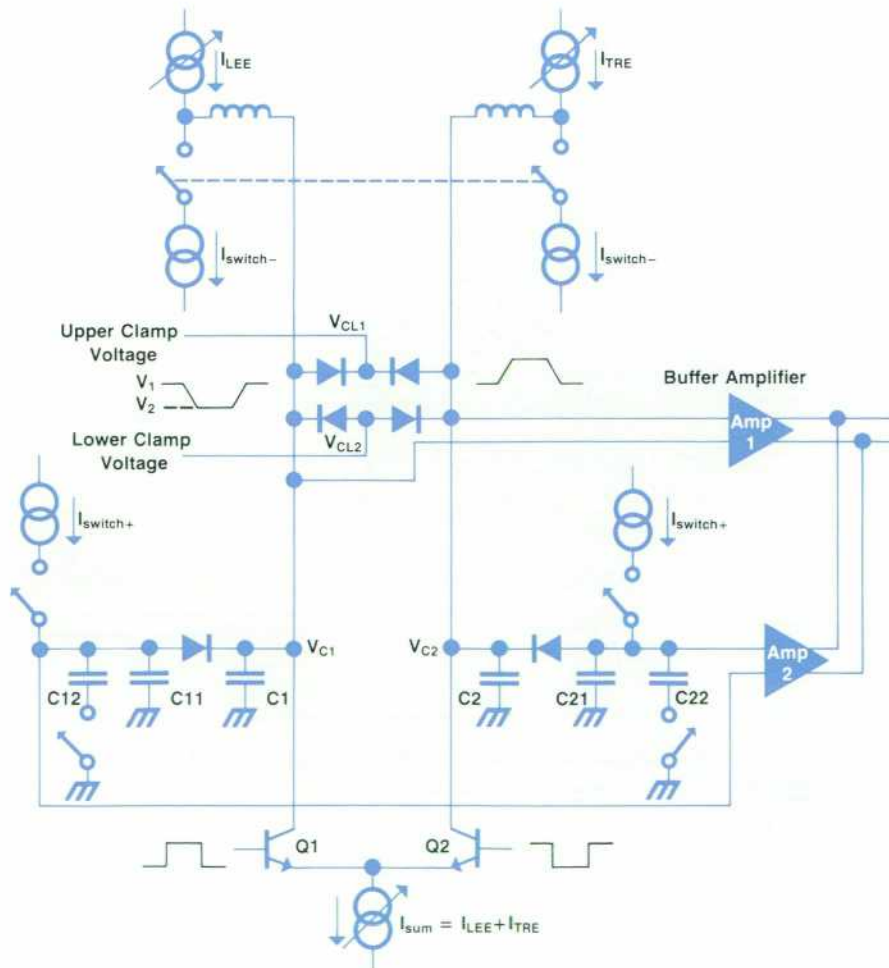


**Fig. 3.** The transition time generator provides programmable transition times from 1.3 ns to 900  $\mu s$ .

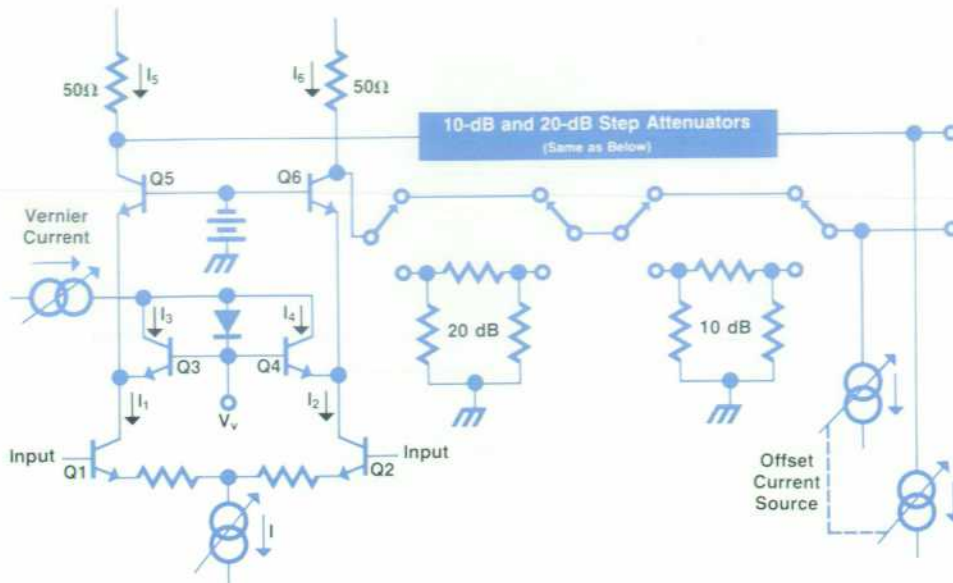


Fig. 4. Output amplifier and attenuator. A dual cascode differential amplifier drives the complementary outputs.

instrument, one output is taken from each channel).

The electronic attenuator consists of a pair of differential amplifiers and a vernier current source. The input signals control the share of current through Q1 and Q2 and therefore the current through each differential amplifier.

Similarly,  $V_V$  controls the current in attenuator transistors Q3, Q5 or Q4, Q6. Assume that  $V_V$  is set to an attenuation factor of 2,  $I = 100$  mA, and the input is such that both  $I_1$  and  $I_2 = 50$  mA. Then  $I_3 = \frac{1}{2}I_1 = 25$  mA and  $I_4 = \frac{1}{2}I_2 = 25$  mA, which adds to a vernier current of 50 mA. The sum  $I_3 + I_4$  remains constant for all input signal conditions with  $I_1$  and  $I_2$  split appropriately so that the remaining currents  $I_5$  and  $I_6$  cause the desired output amplitude at the load resistors. This is true for all attenuation ratios. The active vernier operates over a dynamic range of 10 dB. 10-dB and 20-dB step attenuators can be switched into the signal path for a total amplitude variation of 40 dB, giving an amplitude

range of 50 mV to 5V. Without addition of an offset current source, the output pulses would always be negative. A bipolar current source is added to supply any current value between  $-200$  mA and  $+200$  mA to allow an offset voltage of  $+5$ V maximum. For ease of use, calculation of the amplitude, offset and step attenuator setting is done by the microprocessor. An additional feature in the Option 020 instrument, besides the availability of a second output channel, is the selectable built-in  $50\Omega$  passive adder. In the A-add-B mode, the sum of the output signals is available at the channel A connector and the channel B outlet is disabled. This feature can be used to generate waveforms like fast staircases (Fig.5) and multilevel signals, or for the simulation of glitches, spikes, and overshoot on signals with transition times as low as 1.5 ns (Fig. 6).

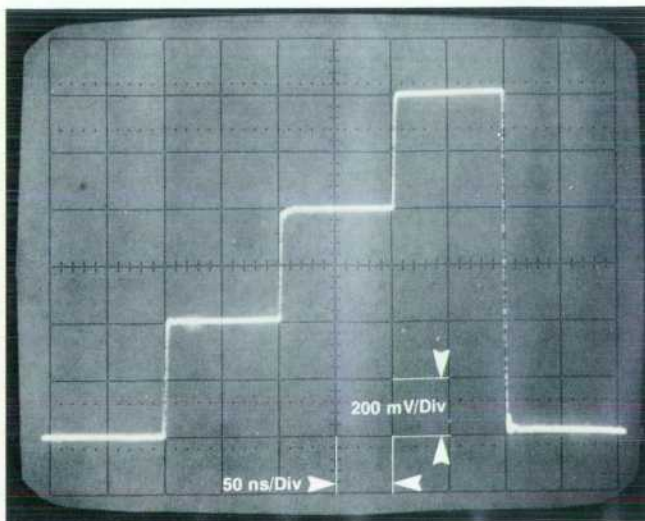


Fig. 5. The 8161A Option 020 can generate fast staircases for testing A-to-D converters, multilevel logic, or pulse-height discriminators.

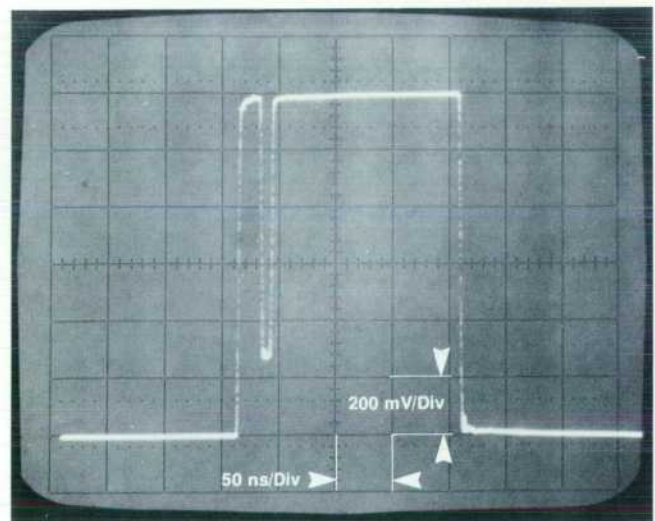


Fig. 6. The A-add-B mode makes it possible to simulate glitches, spikes, and overshoot with transition times as low as 1.5 ns.

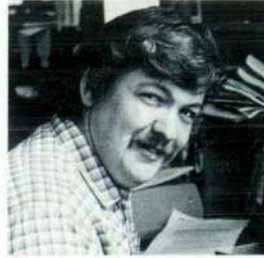
## Acknowledgments

Uwe Neumann contributed the software and the redesign of the microprocessor board. Hartwig Bartl modified the mechanical design to meet RFI requirements. A lot of helpful ideas were provided by lab section manager Werner Hüttemann and product manager Jürgen Brettel.

## Reference

1. W. Hüttemann, L. Kristen, and P. Aue, "A Precision, Programmable Pulse Generator," Hewlett-Packard Journal, May 1979.

## Peter Aue



A Diplom Ingenieur graduate of the University of Stuttgart, Peter Aue joined HP's Böblingen Instruments Division in 1976. Before he became project leader of the 8161A, he contributed to the design of the 8160A timing circuitry. Peter is married, has three daughters, and lives in Böblingen. He spends his spare time working on his house, doing woodwork and building model trains.

## SPECIFICATIONS HP Model 8161A Pulse Generator

### Pulse Parameters (50Ω Load)

#### PERIOD:

RANGE: 10.0 ns to 980 ms.  
RESOLUTION: 3 digits (best case 100 ps)  
ACCURACY:  $\pm 3\%$  of programmed value  $\pm 0.5$  ns (period  $< 100$  ns)  
 $\pm 2\%$  of programmed value (period  $\geq 100$  ns)  
MAXIMUM JITTER: 0.1% of programmed value + 50 ps.

#### DELAY, DOUBLE PULSE, WIDTH: (Specifications apply for minimum transition times, measured at 50% of amplitude. Delay is measured from trigger to main output).

DELAY (DEL) RANGE: 0.0 ns to 990 ms.  
DOUBLE PULSE (DBL) RANGE: 8.0 ns to 990 ms.  
WIDTH (WID) RANGE: 4.0 ns to 990 ms.  
RESOLUTION: 3 digits (best case 100 ps).  
ACCURACY:  $\pm 1\%$  of programmed value  $\pm 1$  ns.  
MAXIMUM JITTER: 0.1% + 50 ps ( $\leq 999$  ns)  
0.05% (999 ns to 9.99  $\mu$ s)  
0.005% ( $> 9.99$   $\mu$ s)

#### DUTY CYCLE LIMITS:

DELAY: for DEL  $\geq 50$  ns, DEL<sub>max</sub>  $< 0.94$  PER - 30 ns.  
for DEL  $< 50$  ns, DEL<sub>max</sub> independent of period.  
WIDTH: for WID  $\geq 50$  ns, WID<sub>max</sub>  $< 0.94$  PER - 30 ns.  
for WID  $< 50$  ns, WID<sub>max</sub>  $< 0.94$  PER - 3 ns.

#### OUTPUT LEVELS:

HIGH LEVEL (HIL) RANGE: -4.95V to 5.00V.  
LOW LEVEL (LOL) RANGE: -5.00V to 4.95V.  
RESOLUTION: 3 digits (10 mV).  
AMPLITUDE: 0.06V minimum, 5.00V maximum.  
LEVEL ACCURACY:  $\pm 1\%$  of programmed value  $\pm 3\%$  of amplitude  $\pm 25$  mV.  
SETTLING TIME: 20 ns plus transition time to achieve specified accuracy.

#### NOTE:

In A add B Mode (Opt. 020 only):  
HIGH LEVEL (HIL) RANGE: -1.75V to 1.80V.  
LOW LEVEL (LOL) RANGE: -1.80V to 1.75V.

#### TRANSITION TIMES (10-90% Amplitude):

LEADING EDGE (LEE): 1.3 ns\* to 900  $\mu$ s.  
TRAILING EDGE (TRE): 1.3 ns\* to 900  $\mu$ s.  
\* $< 1$  ns (20-80% amplitude)

\*1.5 ns in A add B mode (Opt. 020 only).  
LINEARITY:  $\pm 5\%$  for transition times  $> 30$  ns.

**PRESHOOT, OVERSHOOT, RINGING:**  $\pm 5\%$  of amplitude  $\pm 10$  mV for transition times  $\geq 2.5$  ns, may increase to  $\pm 10\%$  of amplitude  $\pm 10$  mV for transition times  $< 2.5$  ns.

**A ADD B:** Adds Channel A and B outputs (Opt. 020).

**OUTPUT FORMAT:** 8161A: Simultaneous normal and complement output.  
8161A Opt. 020: Channel A and B, normal/complement independently selectable.

### Operating Modes

**NORM:** Continuous pulse stream.

**GATE:** External signal enables rate generator. First output pulse sync with leading edge. Last pulse always complete.

**TRIG:** Each input cycle generates a single output pulse.

**BURST:** Each input cycle generates a programmable number (0 to 9999) of pulses.  
Minimum time between bursts is 1 period. Minimum period setting in burst mode is 15.0 ns.

**MAN:** Simulates external signal when EXT INPUT switched OFF.

**SINGLE PULSE:** Provides a single pulse independent of input and period settings.

### General

**RECALIBRATION PERIOD:** 1 year.

**WARM-UP TIME:** 30 minutes to meet all specifications.

**REPEATABILITY:** Factor of 2 better than specified accuracy.

#### ENVIRONMENTAL:

STORAGE TEMPERATURE:  $-40^{\circ}\text{C}$  to  $75^{\circ}\text{C}$ .

OPERATING TEMPERATURE:  $0^{\circ}\text{C}$  to  $50^{\circ}\text{C}$ .

Specifications apply from  $20^{\circ}\text{C}$  to  $40^{\circ}\text{C}$ .

Accuracy derating for temperatures from  $20^{\circ}\text{C}$  to  $0^{\circ}\text{C}$  and from  $40^{\circ}\text{C}$  to  $50^{\circ}\text{C}$  with factor  $(1 + 0.05 \times \Delta^{\circ}\text{C})$ , where  $\Delta^{\circ}\text{C}$  is the temperature deviation outside the  $20^{\circ}\text{C}$ - $40^{\circ}\text{C}$  range.

HUMIDITY RANGE: 95% R.H.,  $0^{\circ}\text{C}$  to  $40^{\circ}\text{C}$ .

**POWER-OFF STORAGE:** After eight hours of operation, batteries maintain all stored data up to 2 weeks with instrument switched off. Hardwired addressable location contains a fixed operating state for confidence check (standard parameter set).

**POWER:** 115/230V rms + 10%, -22%; 48-66 Hz; 675VA maximum.

**WEIGHT:** Net 20.8 kg (46 lbs), Shipping 25 kg (55 lbs).

**DIMENSIONS:** 178 mm high, 426 mm wide, 500 mm deep (7 x 16.8 x 19.7 in).

**PRICES IN U.S.A.:** 8161A Programmable Pulse Generator, \$14,940, Option 020 Second Channel. Includes delay, width, double pulse, transition times, and output amplifier, \$6590.

#### MANUFACTURING DIVISION: BÖBLINGEN INSTRUMENT DIVISION

Hewlett-Packard GmbH  
Herrenberger Strasse 110  
D-7030 Böblingen  
Federal Republic of Germany

Hewlett-Packard Company, 1501 Page Mill  
Road, Palo Alto, California 94304

Bulk Rate  
U.S. Postage  
Paid  
Hewlett-Packard  
Company

### HEWLETT-PACKARD JOURNAL

SEPTEMBER 1981 Volume 32 • Number 9

Technical Information from the Laboratories of  
Hewlett-Packard Company

Hewlett-Packard Company, 1501 Page Mill Road  
Palo Alto, California 94304 U.S.A.

Hewlett-Packard Central Mailing Department  
Van Heuven Goedhartlaan 121  
1181 KK Amstelveen, The Netherlands

Yokogawa-Hewlett-Packard Ltd., Suginami-Ku  
Tokyo 168 Japan

04000940356 && HANS & QM00  
MR Q M HANSEN  
NASA AMES RESEARCH CENTER  
FPD DIV  
CODE BLDG N 244-7  
MOFFETT FIELD CA 94035

**CHANGE OF ADDRESS:** To change your address or delete your name from our mailing list please send us your old address label. Send changes to Hewlett-Packard Journal, 1501 Page Mill Road, Palo Alto, California 94304 U.S.A. Allow 60 days.